# Review Article: Case studies in future trends of computational and experimental nanomechanics

William Gerberich, Ellad B Tadmor, Jeffrey Kysar, Jonathan A Zimmerman, Andrew M Minor, Izabela Szlufarska, Jonathan Amodeo, Benoit Devincre, Eric Hintsala, R Ballarini

# Review Article: Case studies in future trends of computational and experimental nanomechanics

William Gerberich, Ellad B. Tadmor, Jeffrey Kysar, Jonathan A. Zimmerman, Andrew M. Minor, Izabela Szlufarska, Jonathan Amodeo, Benoit Devincre, Eric Hintsala, and Roberto Ballarini

Citation: Journal of Vacuum Science & Technology A: Vacuum, Surfaces, and Films **35**, 060801 (2017); doi: 10.1116/1.5003378

View online: http://dx.doi.org/10.1116/1.5003378

View Table of Contents: http://avs.scitation.org/toc/jva/35/6

Published by the American Vacuum Society

REVIEW ARTICLE

# Review Article: Case studies in future trends of computational and experimental nanomechanics

William Gerberich[a)]
*Department of Chemical Engineering and Materials Science, University of Minnesota, 421 Washington Avenue SE, Minneapolis, Minnesota 55455*

Ellad B. Tadmor[b)]
*Department of Aerospace Engineering and Mechanics, University of Minnesota, 110 Union Street SE, Minneapolis, Minnesota 55455*

Jeffrey Kysar[c)]
*Department of Mechanical Engineering, Columbia University, 500 West 120th St., New York, New York 10027*

Jonathan A. Zimmerman[d)]
*Sandia National Laboratories, Hydrogen and Materials Science Department, Livermore, California 94550*

Andrew M. Minor[e)]
*Department of Materials Science and Engineering and Lawrence Berkeley National Laboratory, Molecular Foundry, National Center for Electron Microscopy, One Cyclotron Rd., MS-72, Berkeley, California 94720*

Izabela Szlufarska[f)]
*Department of Materials Science and Engineering, University of Wisconsin, 1509 University Avenue, Madison, Wisconsin 53706*

Jonathan Amodeo[g)]
*Laboratoire MATEIS, UMR 5510 CNRS INSA-Lyon Université Lyon 1, 7 Avenue Jean Capelle, F-69621 Villeurbanne, France*

Benoit Devincre[h)]
*Laboratoire d'Etude des Microstructures, UMR 104 CNRS-ONERA, 29 Avenue de la Division Leclerc, F-92322 Chatillon, France*

Eric Hintsala[i)]
*Hysitron, Inc., 9625 W 76th St., Eden Prairie, Minnesota 55344*

Roberto Ballarini[j)]
*Department of Civil and Environmental Engineering, University of Houston, N107 Engineering Building 1, Houston, Texas 77204-4003*

(Received 29 December 2016; accepted 26 July 2017; published 25 September 2017)

With rapidly increasing numbers of studies of new and exotic material uses for perovskites and quasicrystals, these demand newer instrumentation and simulation developments to resolve the revealed complexities. One such set of observational mechanics at the nanoscale is presented here for somewhat simpler material systems. The expectation is that these approaches will assist those materials scientists and physicists needing to verify atomistic potentials appropriate to the nanomechanical understanding of increasingly complex solids. The five following segments from nine University, National and Industrial Laboratories both review and forecast where some of the important approaches will allow a confirming of how *in situ* mechanics and nanometric visualization might unravel complex phenomena. These address two-dimensional structures, temporal models for the nanoscale, atomistic and multiscale friction fundamentals, nanoparticle surfaces and interfaces

[a)]Electronic mail: wgerb@umn.edu
[b)]Electronic mail: tadmor@umn.edu
[c)]Electronic mail: kysar@columbia.edu
[d)]Electronic mail: jzimmer@sandia.gov
[e)]Electronic mail: aminor@berkeley.edu
[f)]Electronic mail: szlufarska@wisc.edu
[g)]Electronic mail: jonathan.amodeo@insa-lyon.fr
[h)]Electronic mail: devincre@onera.fr
[i)]Electronic mail: ehintsala@hysitron.com
[j)]Electronic mail: rballari@central.uh.edu

  

and nanomechanical fracture measurements, all coupled to *in situ* observational techniques. Rapid future advances in the applicability of such materials science solutions appear guaranteed. 
[http://dx.doi.org/10.1116/1.5003378]

## I. INTRODUCTION

This contribution utilizes multiple problems in nanoscale mechanics to highlight the need for collaborative studies between experimentalists and theoreticians. The case studies presented here are all part of a greater continuing effort to better understand the flow and fracture of metals, ceramics, and semiconductors. Recent developments of new experimental and computational tools have created new opportunities to study previously inaccessible phenomena. For instance, experimental *in situ* measurements in transmission and scanning electron microscopes (TEM and SEM) at unprecedented scales make it possible to characterize defect nucleation, near atomic-scale defect structure, and defect motion. Such measurements can be made under controlled external conditions such as stress, strain rate, and temperature. At the same time, theoretical developments in spatial and temporal multiscale modeling dramatically increase the size and duration of processes that can be simulated using accurate models for atomic interaction. As a result, for the first time, the range of phenomena accessible via experiments and computations is beginning to overlap. Now is the time for nanoscale experimentalists and theorists to work closely together to advance understanding of the basic nanoscale mechanisms governing the behavior and failure of materials at both small and large scales.

This article presents case studies of different areas where experiments, computations, and theory are coming together to make progress. Recent developments are highlighted, while noting the current limitations and future directions for research. An effort has been made to include researchers from different disciplines including physics, materials science, as well as mechanical, aerospace, and civil engineering, the latter three being involved in continuum, discretized, and computational mechanics. The following case studies are included.

In Sec. II, Jeffrey Kysar reports on the use of applied mechanics predictions based on finite element simulations of 2D structures, which could be comparable to molecular dynamic (MD) simulations. The caution is a need for experimental validation to identify the limitations of macroscopic theory.

In Sec. III, Jonathan Zimmerman and Andrew Minor discuss recent developments in computations and experiments for resolving time scales of deformation. This includes developments in temporal multiscale methods and high-speed measurements in transmission electron microscopy.

In Sec. IV, Izabela Szlufarska and Ellad Tadmor discuss atomistic and multiscale modeling of nanoscale contact at realistic size and loading rates. This enables connections with recent advances in atomic force microscopy (AFM) that help illuminate the fundamental nature of friction.

In Sec. V, Jonathan Amodeo and Benoit Devincre discuss the state-of-the-art in understanding the role of surfaces and interfaces on nanoparticles (NPs), drawing on recent advances in atomistic and discrete dislocation dynamics (DD) simulations enabling direct contact with electron microscopy results.

In Sec. VI, Eric Hintsala, Roberto Ballarini, and William Gerberich discuss how recent advances in *in situ* transmission electron microscopy experiments of nanoindentation and fracture can be combined with theoretical dislocation mechanics to illuminate the brittle-to-ductile transition in nanomaterials.

This is an exciting time in nanoscale mechanics. Breakthroughs in understanding typically happen when experiments and theory come together in new ways. We encourage theoretical, computational, and experimental researchers from all disciplines interested in nanoscale phenomena to take advantage of the confluence of theory and experiments and to collaborate to advance our understanding of the fundamentals of material behavior at the nanoscale.

We reached out to a group of researchers active in cooperative studies based upon experimental and theoretical mechanics which might resolve long standing (friction) or more recent (length and time scale) problems. With that in mind, this communication represents ten authors and seven research establishments addressing the above title.

## II. EXPERIMENTAL VALIDATION OF NONLINEAR ANISOTROPIC ELASTIC CONSTITUTIVE RELATIONSHIP FOR GRAPHENE VIA NANOSCALE INDENTATION EXPERIMENTS

Two-dimensional (2D) materials have been studied intensely over the past decade due to their novel structure and exceptional properties. Graphene—the most well known 2D material—consists of carbon atoms with $sp^2$ hybrid bonding in the form of a monatomically thin hexagonal lattice. It has exceptional thermal[1,2] and electrical[3–5] transport properties as well as the highest strength[6,7] of any known material. Hexagonal boron nitride has the same crystal structure but is an electrical insulator.[5] Phosphorene and silicene are other monatomically thin 2D materials with semiconducting electrical properties. Transition metal dichalcogenides (TMDCs), consisting of three atomic layers, form another important class of 2D materials.[8] The archetypal TMDC is molybdenum disulfide ($MoS_2$), with a monatomically thin hexagonal lattice of molybdenum atoms sandwiched between two monatomically thin hexagonal lattices of sulfur atoms.[9] Other examples include $WS_2$, $WSe_2$, $WS_2$, and $MoTe_2$, which are direct band-gap semiconducting materials.

The exceptional properties of 2D materials present many opportunities to form composites with desirable properties. To that end, van der Waals heterostructures are formed by stacking together various 2D materials selected for their conducting, semiconducting and insulating properties to create new materials with unique optoelectronic properties.[10] Given its immense strength, graphene has been incorporated as a strengthening agent into metals, polymers and ceramics.

Two-dimensional materials are obtained either via mechanical exfoliation from their 3D counterparts[6] or via direct growth with industrially scalable chemical vapor deposition (CVD).[11] Mechanically exfoliated specimens of graphene produced in pristine single crystal form contain no 1D defects [e.g., grain boundaries (GB)] and have a vanishingly small density of 0D defects (e.g., atomic vacancies, substitutions, and interstitials) in the areal bulk away from the free edges. Graphene grown via CVD, however, often contains both 0D and 1D defects.

Two-dimensional materials serve as a test bed for fundamental physics and chemistry due to their 2D nature topology. In addition, the pristine nature of mechanically exfoliated 2D materials such as graphene provides a test bed for the study of the mechanics and mechanical properties of crystalline materials under extreme elastic strains. In this section, we review a set of experiments that characterizes the rupture of pristine graphene. We also discuss a multiscale elastic constitutive model based upon *ab initio* calculations as well as a detailed finite element analysis of the experimental results. We then focus on several unresolved issues related to the experimental validation of the finite element analysis.

Graphene was first isolated in 2005 via mechanical exfoliation. Lee *et al*. performed a set of experiments on freestanding films of monatomically thin pristine graphene suspended over circular wells of 1.0 and 1.5 $\mu$m diameter.[6] The centers of the freestanding specimens were indented up to the point of specimen rupture with different diamond indenter tips having radii of curvature ranging from about 15 to 25 nm using an AFM or a nanoindenter.

For a given specimen diameter, the force versus displacement indentation response is independent of the radius of curvature of the indenter tip. This allows the system to be modeled as a circular membrane loaded by a point force, from which the Young's modulus and the residual tension in the graphene specimens can be determined experimentally. The force on the indenter tip at rupture, however, is a function of the radius of curvature of the indenter tip, but not on the diameter of the specimen. This suggests that the details of the stress concentration in the graphene in the immediate vicinity of the indenter tip plays the decisive role in establishing the indenter force at which rupture occurred for a given tip radius of curvature.

The experimentally observed rupture force in pristine graphene adopts a normal distribution rather than a Weibull distribution that would be expected for a brittle elastic material. Thus, Lee *et al*. postulated[6] the specimens to be free of defects (at least in the ~1% of the specimen area nearest the indenter tip) so that failure occurs at the material's *intrinsic strength* at which the atomic bonds ruptured in the absence of any lattice defects. This imputed a nonlinear elastic response to the graphene. Lee *et al*. then introduced a simple nonlinear elastic model of graphene by invoking an idealized isotropic third-order elastic stiffness and developed a finite element model (FEM) of the experimental configuration.[6] The magnitude of the third-order elastic stiffness was estimated via an inverse analysis of the finite element model. From this approximate analysis, Lee *et al*.[6] and Kysar[12] estimated the intrinsic strength of pristine graphene to be about 100 GPa.

Wei *et al*. developed a multiple length scale nonlinear anisotropic elastic constitutive description for graphene by expanding the strain energy density potential function in a Taylor series in powers of strain truncated after the fifth order term.[13] Upon considering the symmetries of the graphene crystal lattice, they identified 14 independent elastic constants that account for the nonlinearity and anisotropy of the elastic response. They next performed atomic scale density functional theory (DFT) computations of graphene deformed under in-plane *uniaxial strain* and *equibiaxial strain* conditions to finite strains past the critical strain associated with the intrinsic strength.[9] The 14 continuum elastic constants were then determined through a least-squares curve fit of the continuum description to the atomic scale DFT computations. To check the internal consistency of the constitutive model, they predicted the continuum response of graphene to finite deformations under *uniaxial stress* and demonstrated excellent agreement with an independent set of DFT calculations. It bears emphasis that this constitutive formulation accounts only for in-plane tensile deformations. Xu *et al*.[14] and Kumar and Parks[15] have also developed elastic constitutive models for arbitrary tensile in-plane deformation of graphene.

Wei and Kysar then focused on an experimental validation of the multiple length scale constitutive model.[7] They implemented the constitutive model as a User Material (UMAT) subroutine in the context of the general-purpose finite element package ABAQUS. Employing the UMAT, they developed a detailed FEM of the experiments reported by Lee *et al*.,[6] including modeling a range of specimen diameters as well as a range of indenter tip diameters. For boundary conditions, they assumed zero displacements of the graphene at the periphery of the circular specimens and assumed zero friction at the contact between the rigid indenter and the graphene. The predicted force versus displacement response from the FEM analysis was in close accordance with the experimental response. When modeling the failure of an elastic continuum, it is typically necessary to develop and invoke a failure criterion predicated on the existence of material defects independently of the constitutive model. In this case, however, the material is postulated to be pristine so no defects exist for which a failure criterion can be applied. Nonetheless Wei *et al*.[7] demonstrated that rupture of the graphene is predicted by the model based upon an structural instability at which the specimen is unable to store an additional increment of elastic energy associate with an addition increment of loading (via a prescribed displacement rate of the indenter tip). They interpreted this structural instability leading directly to the

catastrophic failure of the graphene specimens observed experimentally.

The FEM model of Wei and Kysar[7] predicts that the material points in the graphene in contact with the indenter tip at the point of structural instability have suffered an elastic strain in excess of the strain at which instabilities are predicted—to be discussed further below. Thus these material points exhibit a negative tangent modulus. Clearly, such deformation states are in an unstable equilibrium and local rupture at smaller indenter forces is forestalled only due to the constraints provided by the surrounding graphene under stable equilibrium and the indenter tip itself. Wei and Kysar[7] introduced a very small amount of effective viscosity to the elastic constitutive model to reduce the numerical instabilities associated with very small positive, zero and even negative tangent moduli, which may also play a role in forestalling rupture in the FEM analysis.

The force on the indenter tip at which the structural instability leads to failure in the continuum FEM simulation is in excellent accordance with the force on the indenter tip at which rupture occurs experimentally. Specifically, the predicted indenter force lies within the confidence interval from the experiments, respectively, for both AFM indenter tip radii employed. Such excellent quantitative agreement between theory and experiment *apparently* provides an experimental validation of both the nonlinear anisotropic continuum description as well as the assumptions employed in the associated atomic scale DFT simulations.[16] However, as alluded to above, other failure mechanisms in graphene have been identified that are predicted to occur at elastic strains smaller than those predicted in the FEM analysis.

Marianetti and Yevick identified a soft phonon mode instability[17]—akin to a phase transition—operating under homogeneous in-plane deformation states that leads to failure at strains smaller than those predicted by the FEM simulations of Wei and Kysar.[7] If activated, this failure mechanism would lead to specimen rupture at an indenter force smaller than that measured experimentally. In addition, Kumar and Parks[15] noted that graphene's acoustic tensor loses its positive definiteness under homogeneous in-plane deformation states at strains smaller than those predicted by the FEM simulations. The loss of positive definiteness implies the activation of an elastic instability that, if activated, would likewise lead to specimen failure at smaller indenter forces.

The apparent suppression of the soft phonon mode instability and the acoustic tensor elastic instability complicates the use of the experiments to validate the constitutive models and various failure mechanisms. It is worthwhile recalling that the constitutive models were developed assuming only in-plane homogeneous deformation states because the contribution to the overall elastic strain energy density due to flexural deformations is negligible compared to the in-plane deformations. Likewise the criteria for the soft phonon mode and the elastic instability failures are predicated upon an in-plane homogeneous deformation state.

The experimental conditions are not as ideal as assumed in the theoretical developments. The deformation state in the graphene in the experiments is highly heterogeneous with potentially significant strain gradients, especially in the region of high stress concentration. Furthermore, the indenter tip is in contact and provides the experimental loading on the specimen via prescribed displacement rates. The graphene conforms to the shape of the indenter tip, which prescribes constraints on out-of-plane displacements in the region of highest in-plane strain and also induces potentially significant out-of-plane flexural deformations. While friction between a spherical diamond tip and graphene has been characterized experimentally by Ref. 18, the frictional loading is not taken into account either in the FEM simulation of Wei and Kysar[7] or in the predictions of failure via soft phonon mode or the elastic instabilities. Since the experiments are performed in a laboratory environment, there is potentially a monolayer of $H_2O$ separating the indenter tip and the graphene film. Finally, the diamond indenters used in the experiments are elastic and consist of $sp^3$-hybrid carbon atoms with tips that only approximate the spherical shape assumed in the FEM simulations of Wei and Kysar.[7] Indeed, Kumar and Parks[19] accounted for the atomic structure and potential atomic interactions between the diamond indenter tip and the graphene film in addressing one potential explanation for the suppression of the instabilities in the experiments.

As is almost always the case for experimental validation, the experiments need to be performed under more ideal conditions and the theories need to be applicable under more nonideal conditions. In the present case, the development of new experimental methods that introduce a more ideal (e.g., in-plane and homogeneous) deformation state would enable a more direct comparison with theory. However, the "real world" deformation states induced in the indented graphene provide motivation for the incorporation of the nonideal into the theories.

## III. RESOLVING THE TIME-SCALES OF DEFORMATION WITH *IN SITU* OBSERVATION AND ATOMISTIC COMPUTATION

Atomistic simulation, and particularly classical MD, is a valuable tool for investigating the nanoscale underpinnings of material deformation. Examples include inelastic deformation and failure of nanowires,[20,21] fracture of brittle interfaces induced by mixed mode loading,[22] delamination of stiff thin films from compliant substrates,[23] deformation of grain boundaries in polycrystalline ductile metals,[24–26] and the behavior of line defects in semiconductors.[27] While these examples are for crystalline materials, they nonetheless demonstrate the huge role that MD can play in understanding materials deformation. This said, MD is well known to be limited in its ability to examine phenomena that occur over large timespans (as compared to the nanosecond regime) that may involve a combination of diffusive and displacive mechanisms. The influence of timescale was demonstrated recently by Smith *et al.*,[26] who showed that the initial active mechanism during deformation of nanocrystalline Tantalum, and the type of defects created (dislocations versus twins), differed significantly as strain rates varied below or above (respectively) $10^8\,s^{-1}$. While diffusion was probably minimal

for the rates examined in the above study, it nonetheless shows that deformation timescale can have a profound impact on modeling predictions.

Approaches to extend the applicability of atomistic simulation to timescales more representative of real-word experiments vary in their complexity, ingenuity, and effectiveness. The earliest advances in this field are the well-known efforts by Voter and colleagues,[28–34] namely, hyperdynamics, parallel replica dynamics (PRD, or ParRep), and temperature accelerated dynamics (TAD). PRD was developed for systems that undergo infrequent events (i.e., atomic motions that act in concert to significantly alter the system's configuration and associated energy) that obey first-order kinetics. Infrequency of events allows multiple copies of the system to be simulated independently, until the first event occurs in any of the replicas. At that time, all other replicas are destroyed, and new ones are created with a duplicate configuration, varying only in their kinematics, effectively restarting the event finding process. For PRD, timescale is enhanced nearly linearly with the number of replicas used. PRD has been used to study stress-driven GB migration[35] and vacancy-induced morphological changes in deformed carbon nanotubes.[36,37] PRD is a robust approach, as it makes no assumptions regarding the types of events that may occur or the nature of any dynamical bottlenecks.[31] Although versatile, PRD is limited in its effectiveness to span timescales, especially for researchers with access to nominal computational resources.

Voter's alternative methods, hyperdynamics[29] and TAD,[32] exploit aspects of transition state theory (TST) to associate events with calculable advances in simulated physical time. For hyperdynamics, including variations such as the bond-boost method by Miron and Fichthorn,[38,39] this amounts to altering the potential energy landscape and is highly effective for phenomena dominated by diffusive mechanisms. In their recent review, Fichthorn and Mubin noted: "a significant advantage of hyperdynamics methods is their capability to resolve the small-barrier problem, which is ubiquitous in materials simulation."[39] They further remarked that more protocols are required in order to correctly formulate boost potentials that effectively treat the "small-barrier problem." For TAD, MD simulations are performed at high temperatures and analyze the probabilities characteristic of the motions/events observed. Methods to identify and compensate for small energy barrier events have been developed for TAD,[33,34] which has increased TAD's efficiency for traversing large spans of simulated time. Applications of TAD include simulating radiation damage and defect stability and mobility in irradiated Mg-based oxides,[36,37,40] as well as the development of compressive strain in metal thin film growth.[41]

The use of TST has also spawned other methods with the potential to accelerate atomistic simulations. Work by Zhu and colleagues[42,43] has developed a modeling framework that computes details of the atomistic energy landscape and utilizes them within TST to develop analytic expressions for thermally activated processes, such as dislocation nucleation. This methodology requires the identification of minimum energy paths (MEPs) that are traversed between pristine and defected states of the material, including the saddle point that characterizes the lowest energy barrier between these states. Techniques such as the nudged-elastic band (NEB) method can be used for such purposes, as was done by Zhu and Li[43] and by Bohner *et al.*[44] Nguyen *et al.* have also used the example of dislocation nucleation at crystal surfaces to study the strengths and limitations of several TST approaches,[45] including both harmonic (hTST) and quasiharmonic approximations of TST as well as a variational-based formulation (VTST). Their results provide physical insight on both the nucleation process at room temperature, and its rate sensitivity. They show that advanced formulations such as the VTST are necessary to correctly predict relative rates between deformation mechanisms, such as vacancy diffusion and dislocation nucleation in a stressed material. However, the computational complexity required by such formulations can be daunting, and the authors suggest a compromise approach (such as using the quasiharmonic approximation of TST) can balance computational cost with prediction accuracy.

Other work on this topic includes that of Delph and colleagues, who combined their method for predicting defect initiation from quasistatic simulation configurations with hTST to generate probabilities for defect initiation at finite temperature and arbitrarily slow loading rates unfeasible by conventional MD.[46,47] A key innovation of this work is to use single-ended methods for identifying and characterizing saddle points, thereby requiring less intrinsic knowledge about the "to be created" defect than in the works mentioned earlier. One method that combines many of these concepts (i.e., hTST, MEPs) with the well-known kinetic Monte Carlo (kMC) approach is that of the equilibrium map (EM) by Pattamatta *et al.*[48] This technique constructs both energetically favorable and unfavorable potential states for a material system using a combination of energy minimization, NEB determination of MEPs saddle points, and hTST, thereby providing a comprehensive picture of possible material deformation outcomes, as well as the relevant theories that can be used to predict probabilities of their instantaneous occurrence. The EM method is a clear example that true progress in resolving deformation over a broad range of timescales can be made by building upon all previous advances, and using combinations in a computationally agile framework.

The approaches discussed thus far share the common feature of using discrete particles (i.e., atoms or molecules) that clearly delineate positions of matter at distinct instances of time. Two alternative approaches are phase field crystal (PFC) and diffusive molecular dynamics (DMD). Developed by Elder *et al.* to model solid transformations at diffusional time scales and atomistic length scales,[49,50] PFC represents atoms by a continuous atomic density field that evolves due to stress and temperature driving forces. PFC is a specialization of the general phase field method, applied at angstrom-to-nanometer resolution to capture characteristics of single to small ensembles of structural defects.[51,52] Because it is a continuum field theory, PFC inherently has the potential to simulate processes that occur over large timespans, such as the nonconservative motion of dislocations, i.e., climb.[53,54] Assessment of the PFC method is ongoing, and concerns

exist regarding the computational expense of using plane wave bases to resolve atomic density in 3D, the limited sophistication of free energy functionals used, the questionable accuracy of the structures and energies predicted for defected states, and the means by which multiparticle correlations could enhance and reformulate these functionals to improve their accuracy.[55] Some complexity has been introduced, such as the binary PFC by Lu *et al.* that uses both number density difference (from liquid state) and phase concentration to simulate boundary migration induced by the Kirkendall effect.[56]

Developed by Li *et al.*, DMD also models coupling diffusional-displacive processes using continuous functions to represent atomic density fields;[57] however, DMD uses Gaussian functions, thereby minimizing the required information needed to represent the material system and deformation-induced defects. DMD can associate spatial points with occupation probabilities of atoms (or conversely, vacancies), and atom types can be varied to represent solutes[58,59] and impurities. Like PFC, DMD does contain issues associated with accuracy that limit its utility as a materials simulation tool. Li *et al.* themselves identified issues such as lack of high-order correlations between atomic sites within the free energy functional used, as well as the need for development of models that "realistically represent the effect of local environment, deformation, and local stress on kinetics."[56] These advances will be needed to make DMD competitive with MD.

The approaches and articles covered here are meant only to provide a context and specific examples of how the research community has extended atomistic simulation to reach the timescale characteristic of most laboratory experiments. While this narrative was not intended to act as a comprehensive review, it nevertheless reveals that the balance between computational efficiency and physical accuracy dictates the degree of "success" that can be attributed to any specific approach. It is probably no coincidence that this same balance is the key issue for atomistic simulation reaching large length scales, as established by the continuing competition between electronic DFT and use of semiempirical interatomic potentials. In addition, while many of these techniques have been applied to crystalline materials, they can also be used to model amorphous structures, such as polymers. The challenge here (particularly with regard to TST-based methods) lies in a significantly larger number of possible configuration transitions, thus potentially limiting the ability for these methods to emulate the behavior of real materials over long times.

The evolution of modern nanoscale[60] and microscale[61] mechanical testing has now made it possible to perform detailed and precise experiments where exact orientations,[62] environments,[63] and stress states[64] can be studied quantitatively and systematically. However, both the spatial and temporal resolutions of these techniques do not yet overlap with those of atomistic simulations. Direct comparison of atomistic simulations with experiments would provide confirmation of simulation results, as well as more helpful interpretation of experimental observations. If this were possible, deformation mechanisms that remain elusive such as the evolution of shear bands, crack tip dynamics, and twin and dislocation nucleation mechanisms could be measured and observed directly without ambiguity. These measurements and observations would allow for the intelligent design of materials that either produced desirable defect dynamics or resisted undesirable ones. However, our current ability to experimentally observe defect interactions and the evolution of deformation structures at the atomic scale is still in its infancy, with only quasistatic observations standing in for the dynamics of true atomic-level rearrangements. The main technical hurdles lie not in our ability to interrogate materials with atomic level precision, but in our ability to observe deformation with high spatial resolution at the true speed of defect nucleation and propagation.

Defects and crack tips in materials move at velocities that depend on the inherent lattice friction, the temperature, and the stress driving them. But in terms of the fundamental physics, the most important regime is at high stresses, where defect nucleation at stress concentrations or defect-defect interactions occurs in high stress fields relative to the bulk flow stress of a sample. At high stresses, dislocations and crack tips will move at the shear velocity in a material, or even higher.[65–67] This leaves us with a fundamental conundrum in terms of individual defect-level observations: how can one observe something as small as a defect moving on the order of the speed of sound? Fundamentally, we must match the speed and spatial resolution of our characterization technique with the speed and spatial extent of our critical defect. For nanometer-scale defects, this means nanosecond-timescales with nanometer spatial resolution.[68,69] The spatiotemporal techniques currently available are primarily ultrafast diffraction techniques, which inherently average information over the field of view. However, understanding deformation phenomena requires a spatially resolved characterization technique that can discern inhomogeneous samples containing defects, cracks, boundaries, and multiphase components. Major initiatives in electron and x-ray imaging of materials are required to push into the spatiotemporal regime that can observe deformation phenomena at atomic-scale in real time. Coupled with established *in situ* techniques for observing deformation in materials, the result will be direct measurement of quantities that can be used in models and direct validation of deformation mechanisms at atomistic levels.

Understanding the nucleation of defects is critical for our understanding what limits the strength and deformation of materials in extreme environments. Heterogeneous nucleation of dislocations, twins, and cracks can depend on local stress concentrations or chemical inhomogeneities that are only accessible with high-resolution electron microscopy and spectroscopy. For example, stress-corrosion cracking (SCC) is a process by which local corrosion at a crack tip leads to brittle failure of metals that would be otherwise ductile. The process of SCC is thought to be strongly influenced by the formation of thin interfacial films, in this case of metal-oxides, ahead of the crack tip.[70–72] However, many outstanding questions remain concerning the mechanisms by which these interfacial oxides form and how they contribute to the dramatic reduction in fracture toughness. Specifically,

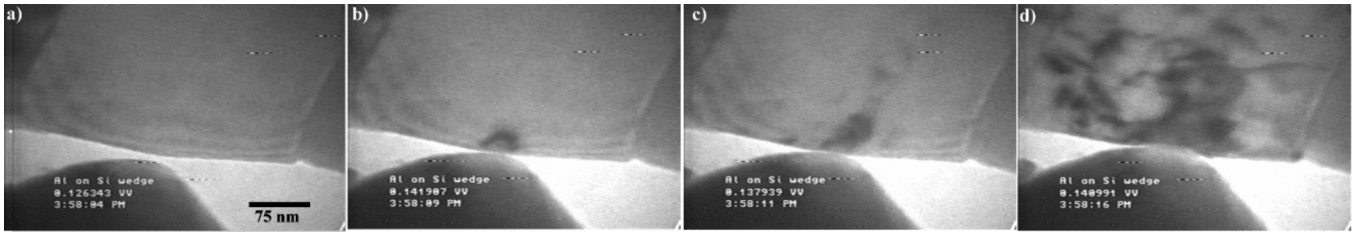


FIG. 1. Nucleation of dislocations in grain of aluminum taken at 30 frames per second. Reprinted with permission from Minor *et al.*, J. Electron. Mater. **31**, 958 (2002). Copyright 2002 by Springer.

these oxides have been observed to form with fast kinetics, adopting metastable crystal structures that are not observed on free surfaces of the same material. The ability to look with atomic resolution at the structure and chemistry of these films and the location of crack initiation, in an environment, under stress, and at ultrafast speeds would lead to fundamentally new insight in this important field. A further example of a mechanical nucleation phenomenon is the sensitivity of local chemistry and stress on the nucleation of dislocations (Fig. 1).[73] The nucleation of dislocations occurs at stress levels on the order of the ideal strength of a crystal. There is substantial interest in understanding the ideal strength of materials, as this provides an upper bound on the achievable mechanical behavior.[74–77] Since dislocations at near theoretical strengths travel at the speed of sound or higher, nanosecond time resolution with atomic resolution is required to capture the subtle atomic-level characteristics that influence the nucleation of dislocations.

## IV. FUTURE OF ATOMISTIC AND MULTISCALE MODELING OF NANOSCALE CONTACT

Mechanics is governed by contact. Physical bodies interact with each other through short-range forces that are idealized at the continuum level as distributions of traction (force-per-unit-area).[78] The continuum approach is powerful and has yielded tremendous insight into contact phenomena. However, in recent years, the focus has shifted to understanding the nanoscale underpinning of macroscopic contact mechanics with an aim to engineer contact properties from first principles. Engineering surfaces are often rough at multiple length scales, and at the smallest length scales, contact consists of asperities that are tens to hundreds of nanometers (nm) in size. Studies at the level of a single nm-sized asperity allow scientists to isolate and quantify specific mechanisms that govern deformation, friction, and wear because it is possible to control with a high degree of precision such parameters as contact geometry, surface and environmental chemistry, and temperature.[79] Of course, a nanoscale perspective is also needed in nano- and microsystems where nanoscale phenomena can dominate the mechanical response. This can become important in manufacturing decisions of how to minimize frictional contact wear by applying low frictional coatings to conductive pathways.

The first studies of contact were undoubtedly empirical. Humans were making stone tools as early as 2.5 million years ago. They were expert at striking quartz, obsidian, and flint with hard rocks to create flake tools. These abilities evolved over time to create impressive feats of engineering based on trial and error. Theoretical contact mechanics can trace its roots back at least to Leonardo Da Vinci in the 15th century who proposed the first friction laws, later rediscovered by Guillaume Amontons. A rigorous mathematical theory for contact of continuum bodies began with Heinrich Hertz's classic paper on the frictionless contact of two curved elastic solids published in 1882. In the nearly 150 years since Hertz, continuum modeling of contact has greatly extended accounting for more complex geometries, friction, inelastic contact and wear, rolling conditions, dynamics, and thermoelastic effects.[80] Of particular relevance to nanoscale contacts are models that include adhesion[81] since at these small scales van der Waals forces can play an important role in deformation. Coupling between individual asperities and their cumulative contribution to contact deformation can be described by multiscale theories and models of rough contacts, which continue to be developed and refined.[82,83]

Continuum contact mechanics is by definition a *phenomenological* theory. By this, we mean that the mathematical models used to describe material behavior and failure are inferred from experiments for specific phenomena of interest. While this is a very effective approach for engineering design, it lacks predictive capability for new phenomena. Thus, continuum theory can be used to design a disc brake assembly, but cannot be used to reengineer the pad and disc materials to increase the friction coefficient. Modeling materials in this fashion requires a more fundamental understanding (both from simulations and experiments) of material interaction down to the atomic or even the quantum level.[84] One of the grand challenges in the field of nanomechanics is to develop predictive models for contact from first principles. For instance, in the case of sliding contacts, there are many mechanisms that can contribute to frictional energy dissipation, and which mechanism is active depends on the properties of the two materials in contact as well as on the external conditions (e.g., sliding speed, normal load, humidity, and so on). In many cases, mechanical response is governed by the evolution of contact during loading (normal and/or shear), and therefore, there is an urgent need for the development of *in situ* experimental techniques and models capable of capturing dynamic evolution of buried interfaces. There are many open questions that need to be addressed; how is the evolution of the microstructure (e.g., grain growth) affected by contact loading and conversely how microstructural changes impact the measured forces? How are mechanical forces coupled to interfacial chemical

reactions under nonequilibrium conditions of dynamic loading? What is the relative contribution to wear from atomic attrition versus the contribution from bulklike plastic deformation (e.g., dislocation motion in crystals)? Atomic attrition refers to the removal and transfer of individual atoms across the contact interface [see Figs. 2(a) and 2(b)].[85]

While knowledge gained from nanoscale single asperity studies can often be transferred and utilized for design of mechanical response at the micro- and macroscale, it is also possible that entirely new phenomena emerge when the contact size is decreased to the nanometer regime. For instance, it has been shown that continuum models of contact may break down at the nanometer length scale[86] and it has been proposed that such small contacts are better described by roughness theories with an asperity being equivalent to a single atom or group of atoms.[87] Contact size can also affect the dominant deformation mechanisms. For instance, in nanoscale contacts, ceramics can deform by means dislocation plasticity (instead of fracture) and can be worn in a ductile manner just like metals [Fig. 2(c)].[88] Effects of small contact size can be coupled to the effects of nano/microstructure. For example, depending on the size of contact relative to the grain size, wear rate and hardness can be either correlated (as in the Archard's law) or uncorrelated with each other.[89]

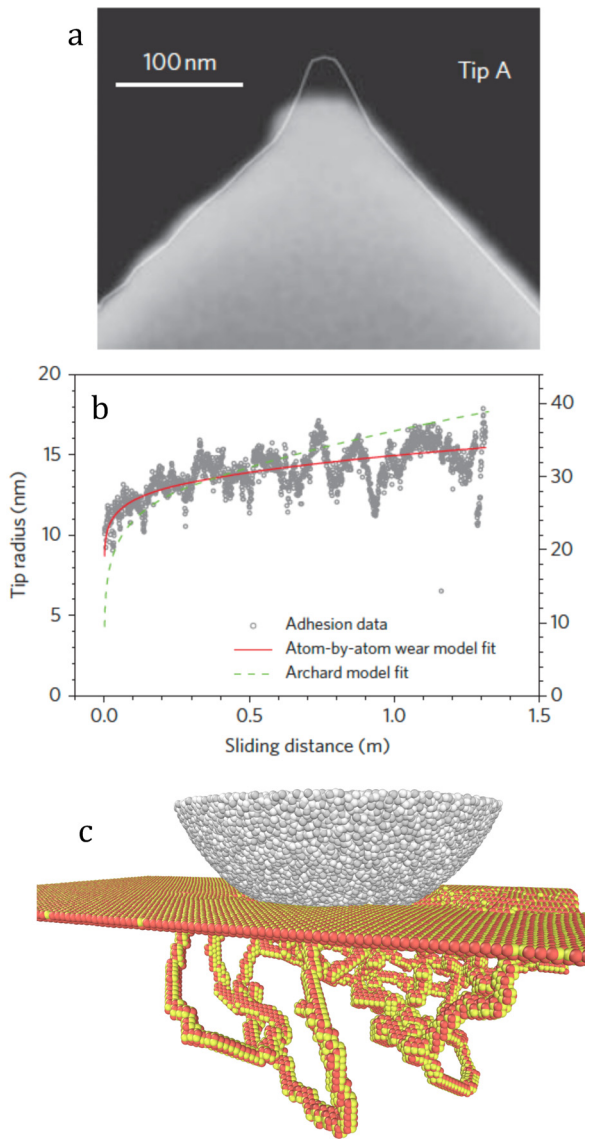


FIG. 2. (Color online) Wear of nanoscale contacts by different mechanisms: (a) scanning electron microscopy image of silicon-containing diamondlike-carbon tip after sliding on $SiO_2$ with the outline of the unworn tip. Adapted with permission from Bhasharan *et al.*, *Nat. Nanotechnol.* **5**, 181 (2010). Copyright 2010 by Macmillan Publishers Ltd. (b) Corresponding change in tip radius as a function of sliding distance measured experimentally (gray points). Atom-by-atom wear model (red) fits the data better than the Archard model (green). Adapted with permission from Bhasharan *et al.*, *Nat. Nanotechnol.* **5**, 181 (2010). Copyright 2010 by Macmillan Publishers, Ltd. (c) MD simulation of a rigid AFM tip sliding on SiC show dislocation plasticity as the main deformation mechanism (Ref. 88).

Atomistic simulations, based on either approximate classical force fields[78,90] or more accurate quantum mechanics,[91–93] have greatly contributed to fundamental understanding of contact behavior at the nanoscale (see, for instance, Ref. 78 for a review). In such simulations, the materials coming into contact are treated as a collection of atoms and their dynamics are obtained by integrating Newton's equations of motion subject to constraints that impose macroscopic boundary conditions such as pressure and temperature.[83] This is referred to as MD. In principle, simulations of this type are predictive and can be used to explore the sort of open questions listed earlier. However, there are limitations. First, the predictive ability of a simulation that uses a classical interatomic model or force field (which is normally a necessity given the very high cost of quantum calculations) is entirely tied to the fidelity of the model. Determining the *transferability* of such models, i.e., their ability to predict behavior that they were not fitted to reproduce, is a challenge in atomistic modeling, and one of the main objectives of the recent Open Knowledgebase of Interatomic Models (https://openkim.org) project.[94]

A second limitation of MD is tied to the size of calculations that can be performed. Even with the availability of high-performance computing, there remain disparities in length and time scales between atomistic simulations and experimental systems. For example, for a realistic potential energy function, the practical limit on the number of atoms that can be simulated is on the order of tens to hundreds of millions of atoms.[86,88,95] This system size is sufficient to model contact between a surface and the apex of the tip in AFM experiments,[88,94,96] but not the entire tip and remaining system. Naturally, these length scales are also too small to model micro- and macroscale contacts. The time scale limitation of atomistic simulations is even more severe with the overall simulation time accessible to conventional MD simulations being on the order of one microsecond. These limitations imply that most MD simulations are performed at rates that are several orders of magnitude faster than those used in actual experiments. For example, most AFM experiments are conducted at sliding velocities of hundreds of nanometer per second to a few micrometers per second while conventional MD simulations are performed at a few meters per second.[97–99] Consequently, the deformation mechanisms observed in MD simulations may differ from those that are active in experiments.

In order to overcome the problems of scale disparity, two classes of "multiscale" methods have been developed: *spatial* multiscale methods that combine continuum and atomistic approaches within a single framework and *temporal* multiscale methods that accelerate time in atomistic simulations.[77,100] Early developments of spatial multiscale methods include the static quasicontinuum (QC) method[101,102] and its dynamic finite temperature version called "hot-QC."[103,104] Following QC, a number of similar spatial multiscale methods were developed which differ in the details of how the atomistic and continuum regions are coupled (these methods fall into the class of *coupled domain* approaches), many of which are reviewed in Refs. 83, 105, and 106. In the QC method, regions which contain atomic-scale defects such as dislocations or nanocracks or that experience deformation varying on an atomic length scale are treated fully atomistically, while the remainder of the model is treated more efficiently by adopting the continuum approximation within a finite element method (FEM) framework using the Cauchy–Born rule to obtain the constitutive response. An example is shown in Fig. 3 of a QC model for an AFM simulation. The AFM tip apex and nearby substrate are modeled atomistically, whereas the rest of the AFM tip, AFM beam, and substrate are modeled using an FEM approximation.

The second class of multiscale methods—*temporal multiscale methods*—attempt to address the limited time scale accessible in MD simulations. A number of powerful algorithms have been developed for cases where one can separate the time scales between frequent events (e.g., vibrations of atoms) and rare events, such as hopping of atoms from one metastable state to another. These include hyperdynamics,[28,29] the parallel replica method,[30] and temperature-accelerated dynamics (TAD).[32] In particular, parallel replica[107] and hyperdynamics[108] algorithms have been successfully applied to study friction in nanoscale contacts. However, these methods (in particular hyperdynamics) require the ability to define a rare-event at the contact interface, which is often not possible, and which means that these methods are applicable only to a subset of contact problems. In another approach to accelerating atomistic simulations, a combination of kinetic Monte Carlo and density functional theory was used to describe chemical bonding of contact interface over the time span of hundreds of seconds.[109] Long-time scale chemical evolution can be also described by so-called multibond models.[110]

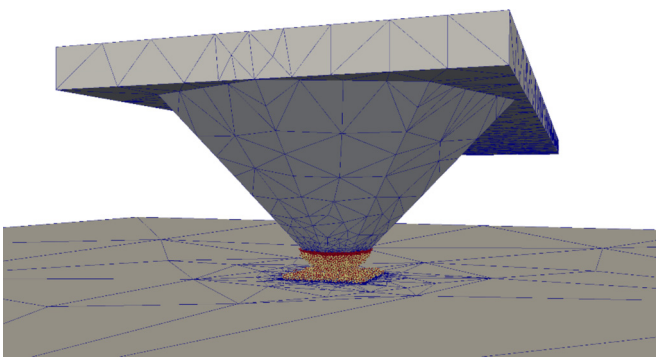

FIG. 3. (Color online) QC model of an AFM contact.

These models at present are phenomenological but, in principle, they can readily accept input from atomistic simulations. Finally, methods based on fluctuation dissipation theory have also been developed to model viscous friction in the limit of extremely low shear rates (long-time scales).[111,112] All of the above mentioned methods have their strengths and limits of applicability, and currently, there is no single method that would allow modeling a general contact problem on experimentally relevant time scales.

Up until now, spatial and temporal multiscale methods have been developed largely independently, and so the *simultaneous* spanning of length and time scales remains one of the great open challenges in multiscale modeling. Recently, a QC method that spans multiple length scales *and* extends the accessible time scale, called "hyper-QC," has been proposed.[113] Hyper-QC combines hot-QC and hyperdynamics within a single framework. In hyperdynamics, a modified potential energy function is used to reduce energy barriers and thereby accelerate the escape from metastable states without altering the characteristics of the original dynamics. The hyper-QC method has been applied to nanoindentation simulations (kinematically constrained to 2D deformation fields) where acceleration factors up to 5000 were obtained.[114] This enables simulation of loading rates only 2–3 orders of magnitude higher than experiment, whereas MD simulations of nanoindentation are normally at least 6 orders of magnitude too fast. Hyper-QC is currently being extended to full 3D and optimized to make it possible to approach even closer to experimental conditions. Temporal acceleration of QC using parallel replica and TAD, which may be more suitable for some contact problems, is also being pursued.

Atomistic and multiscale simulations of nanoscale contacts are already at the point where it is becoming possible to reach not only qualitative, but also a quantitative agreement with experiments. Nevertheless, further developments are needed to continue bridging the time- and length-scale gaps between the two approaches for general contact problems. Among hierarchical multiscale models, atomistically informed kinetic Monte Carlo and multibond models are particularly promising for simulating coupling between contact chemistry and mechanical stresses. Another important area of future developments is modeling nano/microstructural evolution of materials in mechanical contacts. In this regard, multiphysics models that combine finite element analysis, dislocation plasticity, and phase field and that incorporate fundamental understanding and parameters derived from MD and quantum mechanical calculation can provide a powerful approach to such problems when the material's structure evolves on the length scales of micrometer's or larger. For nanoscale contacts, this evolution could be captured using concurrent multiscale models, such as the aforementioned QC method. Theoretical foundation for accelerating time scales of simulations has been already developed for the case where dynamics is governed by rare events. However, new theories and algorithms are needed to model more general contact problems. An example where rare events might not be easily identifiable is sliding at the interface between amorphous or chemically

passivated materials where the contact area includes more than tens of atoms.

## V. MECHANICS OF NANOPARTICLES: A PERSPECTIVE CROSSING ATOMISTICS, DISLOCATION DYNAMICS, AND EXPERIMENTS

This section deals with a multiscale prospection of the mechanical properties of nanoparticles and their nanostructured relatives based on simulations and experimental nanomechanical tests. We will focus on the role of surfaces upon elastic and plastic deformation, but also on interfaces like nanotwins and grain boundaries. Special attention will be paid to the strain conditions driven by dislocations dynamics. This section will cover mechanical properties controlled by dislocation nucleation at surfaces like in nanoparticles, dislocation absorption, and emission from grain boundaries like in nanopolycrystals. The main goal of this prospective is to underline the current strengths and weaknesses, capabilities, and limits of existing investigation methods on nanomaterials deformation.

Among the different nano-objects, NPs could be the one with the highest amount of functionalities. Indeed, they are already used in various domains of application as, e.g., in NEMS, detectors, and biological sensors.[115,116] In all these cases, NPs phase stability and their thermomechanical properties play key roles to ensure their functionality. In the last years, numerous research groups have focused on the development of nanomechanical tests following two main routes: experimental testing assisted by SEM and TEM and atomistic simulations (mostly MD), which are believed to be the more suited techniques at such length scales. The most recent studies deal with metals,[117–120] ceramics/oxides,[121,122] semiconductors,[123–125] and amorphous materials.[126,127] The size of NPs ranges from clusters of 1–5 nm radius up to few hundred nanometers. They may have different shapes (e.g., spheres, icosahedron structures, truncated octahedrons, etc.) due to both the elaboration conditions and the material surface energy.[128,129] In the first subsections of this chapter, a short overview of the NPs original mechanical properties is made. Then, the discussion is extended to small interfaced systems. Finally, emphasize is laid on the weaknesses of the existing methods, and some future directions for investigation are proposed.

When going deep into the submicronic-scale, nano-objects withstand stresses up to a significant fraction of their ideal strength without irreversible relaxation. Thus, large elastic strains up to $\sim$10% are regularly observed opening a route toward *elastic strain engineering* (ESE).[130] The most known and commercial ESE application is strained-silicon technology. Reducing the size of nano-objects postpones the end of the elastic domain, which becomes nonlinear, i.e., stress strain curves show a quadratic shape over several percentages of elastic deformation. Furthermore, it also changes the amplitude of the elastic moduli and thus the dislocation properties through dislocation line energy variations. The size-dependency of elastic properties is generally attributed to the combination of surface excess free energy and nonlinear core phenomena.[131–133] Both of them influence elastic moduli variations: the smaller the system, the more the effective moduli differ from their bulk counterpart. Atomistic simulations show significant variations of the effective elastic moduli below 10–15 nm sized NPs only,[134] while changes are still observed at rather greater sizes in the experiments (see, for example, Mook *et al.*[135]). Many differences between the two approaches need to be explained, and there is still no method to predict the evolution of elastic moduli due to size diminution for a given material (see Gerard and Pizzagalli for quantitative examples[136]). These features can have a major impact as, e.g., in NEMS for which mechanical properties and, in particular, the material strength strongly constrains electronic-based functionalities. Nevertheless, while possible mechanisms for size-dependent elastic properties have been proposed in the literature, a consensus is still lacking. Therefore, a better understanding of nanoscale elasticity through a predictive approach figures as a critical issue for modern mechanical theories.

In the case of low friction forces, the shear stress required to initiate bulk flow in metallic materials is in the order of $\mu/1000$ at room temperature, where $\mu$ is the shear modulus. However, this is not true anymore at the nanoscale where single crystalline samples are known to yield at about $\mu/10$. In massive materials, dislocations accumulate and multiply close to bulk defects which act as energy concentrators. The plastic shear $\gamma_p$ produced by the glide of a dislocation is defined by $\gamma_p = bA/V$, where $A$ is the mean free area swept by the mobile dislocation, $V$ the volume of the sample, and $b$ the Burgers vector magnitude (the elementary shear carried by the dislocation). Hence, the amount of shear produced by a single dislocation in a bulk material is constrained by the ratio, and plastic deformation has to be taken as a collective process to make sense. On the other hand, decreasing size increases the ratio. While this makes dislocation glide more efficient, it emphasizes the discrete nature of plastic shear. As a first consequence, metallic single crystal micropillars below tens of micrometers diameter exhibit a mechanical size-effect that is characterized by a more stochastic flow, an increased yield strength, and a stronger scatter in yield strength with decreasing sample diameter. This is explained by the reduced number of dislocation sources,[137] dislocation exhaustion,[138] source truncation,[139] and dislocation starvation mechanisms.[140] This versatility makes the interpretation of mechanical tests even more sophisticated than in bulk conditions. Furthermore, nano-objects are characterized by a higher surface-to-volume ratio than bulk- and micro-objects that requires accounting for surface and image forces. Gryaznov *et al.*[141] evaluate the critical size below which a dislocation is dragged out from a small particle due to image forces as where $\phi$ is the friction stress. A rough calculation including a friction stress of 50 MPa for iron at room temperature leads to 400 nm. This simple calculation shows the key contribution of image forces to the plasticity of NPs. Following the previous arguments, the lack of a predefined dislocation microstructure is more and more emphasized for decreasing sample sizes down to the nanoscale. NPs are generally considered as pristine (dislocation-free) due do their

size, and hence, dislocation nucleation from the surfaces occurs as the most efficient mechanism for plastic deformation. Some examples inferred from MD simulations are presented in Fig. 4. Both MD simulations and *in situ* TEM confirm this hypothesis. Nevertheless, surface state and the concentration of surface steps could still play an important role on the first episodes of plastic deformation.[142,143]

The dislocation-based nucleation process is responsible for the high shear strength of about $\mu/10$ observed in experimental and simulated NPs compression tests. This result is well illustrated in the seminal work of Alivisatos dedicated to the compression of Au micro- and nanoparticles.[116] The early stage of NPs plastic deformation is ruled by at least three different nucleation processes: the nucleation of partial and/or perfect dislocations in addition to the emission of nanotwins. Van Swyghenoven and colleagues[144] showed that the ratio between unstable and stable stacking fault energies $\gamma_{usfe}/\gamma_{sfe}$ governs the predominance of partial or twinning dislocation nucleation processes at GBs using the generalized stacking fault (GSF) concept. In addition, the partial versus perfect dislocation problem can be solved using both the GSF curves plus a geometric and size-dependent criterion.[145,146] This method is used to interpret and predict occurring elementary processes that also applies for dislocation nucleation in NPs.[120,147] Finally, one additional feature of the plastic deformation regime of NPs is that fracture is generally less common and a brittle-to-ductile transition often occurs.[148,149] The fact that decreasing size induces *the impossibility of comminuting small particles by compression*[150] is a long-time-known phenomenon that however makes more sense looking at the stability of NPs functional properties. This new fracture *nanotoughness* can be several times higher than its bulk counterpart, what favors large deformation processes to take place.

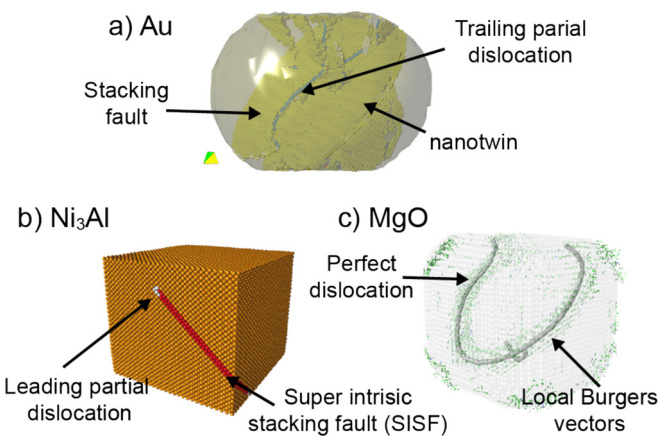


FIG. 4. (Color online) Dislocation-based nucleation processes in NPs as shown by MD simulations. (a) Nucleation of Shockley partial dislocations and deformation nanotwins in a Au fcc nanosphere. Atoms in yellow refer to stacking fault environments. The blue line is a reconstructed trailing partial dislocation. Perfect crystal atoms are removed for convenience (b) Nucleation of a $1/6\langle 112\rangle$ partial dislocation in a $\gamma'$ $Ni_3Al$ nanocube. Atoms in red refer to those in a super intrinsic stacking fault (SISF) environment. Atoms colored in orange refer to a perfect crystal and those in white to the dislocation core environment. (c) Propagation of a perfect $\frac{1}{2}\langle 110\rangle$ dislocation in a truncated MgO nanocube. Green arrows refer to the local Burgers vector distribution at the atomic scale and the gray curve is the reconstructed dislocation.

As a summary, the plastic deformation of NPs generally starts with the nucleation of dislocations from surfaces, vertices, and edges under high stress (>1 GPa). Nanotwinning is also frequently observed. NPs generally show high ductility, even in the case of originally brittle materials. Their amazing fracture toughness appears as a key property, which would require further investigations in the future, especially in the field of theoretical fracture mechanics. The possible formation of dislocation microstructure during plastic deformation has rarely been discussed up till now.[120] This requires more consideration as it could influence NPs mechanical properties and, at a larger scale, have a direct impact on the processing or the design of nanostructured bulk-materials.

From the authors' knowledge, no experimental investigation has yet been made on the mechanical properties of interfaced NPs, except in the case of multifold twinned NPs.[151,152] Thus, the influence in the experiment of twin boundaries (TBs) or GBs has only been postulated from tests made with bicrystalline micro- or nanopillars built from FIB machining.[153–155] Interestingly, it was shown that the presence of an interface in a metallic micropillar does not affect strongly the mechanical properties. In brief, the existence of interfaces essentially helps potentially the dislocation storage by reducing dislocation mean free path and therefore promotes dislocation–dislocation interactions and dislocation multiplication. For an impenetrable boundary such as a high-angle GB, geometrically necessary dislocations accumulation would be expected leading to a Hall-Petch effect. Yet, the formation of a dislocation pile-up is not observed in samples smaller than tens of micrometers diameter. Rather, it was found that GBs act as sinks and sources of dislocations at flow stress larger than 0.5 GPa.[152] Hence, in nano-objects, GBs do not act as a significant barrier to dislocation glide. Indeed, the GB hardening effect associated with the decrease in the dislocation mean free path is counteracted by a new role of the GBs, which act as additional sites of dislocation nucleation in the crystal. It is confirmed by both the higher frequency and smaller magnitude of strain bursts in bicrystalline nanopillars, rather than in single crystalline pillars. Also, the increase in strength observed in bicrystals is not as pronounced as expected from the reduction in single-armed source length. TEM observations also show that the existence of a GB facilitates the annihilation of the dislocations at nearby free surfaces.[153] When there is lack of dislocation accumulation at interfaces, hardening in nanointerfaced materials is primarily governed by a limitation of available dislocation sources. The effect of introducing more than one interface in nanocrystals can also be anticipated from experiments made on polycrystalline microbeams. In such systems, the ratio between free-surfaces and GBs is investigated by reducing the microbeams' dimensions at constant grains size in a bamboo microstructure. In summary, the more the sample contains GBs in a given volume, the larger is the material yield strength and ductility.[156] This effect has also been emphasized in recent MD simulations of nanotwinned NPs.[157] Indeed, growth, deformation, and annealing twins can also provide internal boundaries

which have better thermal and mechanical stabilities than traditional GBs and allow significantly higher ductility.[158,159] The use of model simulations with simplified geometries to analyze dislocation versus TBs interactions[160,161] could help to avoid the size limit of MD simulations of NP compression tests. While the dislocation versus TBs interaction mechanisms are still under debate, the contribution of thermally activated processes like dislocation cross-slip in the vicinity of nanotwins and GBs is shown experimentally and again helps in the formation of additional dislocation sources.

Finally, DD simulations are expected to be an attractive modeling tool to investigate interfaced materials as the latter are necessarily quite large (>100 nm) and can thus not be rigorously studied with atomistic simulations. Nevertheless, the use of DD simulations to study the plasticity of NPs and their interfaces would be useful for critical dislocation properties to be precisely accounted for. This last point echoes one of the possible trends designed to better understand NP mechanical properties in the future as detailed in Sec. IV.

While simple simulations might miss parts of the physics that control NP deformation processes, experiments and limited data may contain biases that can strongly influence our understanding of the mechanical properties of nano-objects. Therefore, a statistical approach of nanomechanical testing is mandatory to avoid biases and nonphysical size-effects. This is particularly well addressed in the study by Mordehai *et al.*[117] where both a wide range of sizes and a huge number of tests are performed. In line with this approach and to conclude this perspective paper, here we propose a list of experimental and simulation points which deserve investigations of NP mechanical properties.

### A. Surface reconstruction and oxidation

Surfaces act as dislocation nucleation sources and sinks in NPs. However, surface atoms rearrange differently than in bulk in several materials (e.g., Si and Au) in order to relax the surface strain and minimize the surface excess free energy. This phenomenon can lead, for example, to surface oxidation that is observed in the TEM as a thin contrasted layer at the surface of the NPs. While some metals such as Au are known to be highly resistant to corrosion, it is not the case for others like, e.g., Fe, Cu, or Al. These *coatinglike* layers are rarely discussed while they could have an influence on the dislocation nucleation process as well as on the starvation process in nano-objects as shown, e.g., in Si nanowires (NW).[162]

### B. Measurements and interferences

The smaller, the more sensitive. Vibrations can strongly affect mechanical data, and TEM imaging of NP compression tests with improved diagnostics should be a continuous task. In a recent paper, Wagner *et al.*[163] underline that vibrations on the *in situ* TEM Hysitron Picoindenter system can induce a 0.1 strain bias measurement on the deformation of 30 nm Si crystals. This has considerable influence on the associated stress level for dislocation nucleation and should receive more attention in the future.

### C. e-beam effect

During *in situ* deformation inside the TEM, samples are subjected to electron bombardment. Zheng *et al.* first show the effect of moderate electron beam exposure on elastic and plastic deformation of amorphous silica NPs and NWs.[164] A qualitative analysis of beam-off versus beam-on data is provided. This phenomenon has been reproduced and quantitatively investigated in terms of irradiation dosage by Mackovic *et al.* However, very little is known about the influence of electron bombardment in crystalline materials, especially in the case of NPs.

### D. Crystal misalignment

The role of the misorientation on the deformation of small-scale objects is a long-term investigated problem as, e.g., in the case of micropillars. Soler and Aldareguia show that misalignments induce significant changes in the flow stress of LiF micropillars.[165] In the case of NPs, Issa *et al.* investigate the mechanical properties of MgO perfectly shaped ⟨001⟩-nanocubes and emphasize the benefits of such geometry compared to the use of nanospheres (e.g., on the slip system analysis).[120] Setup alignment and sample orientation characterization are crucial to correctly measure mechanical properties and rigorously identify elementary processes of deformation.

### E. MD simulated size and strain rate

Besides the well-known MD interatomic potential question, size and strain rate are the two most important weaknesses of MD simulations of nanomechanical tests. Indeed, the size of modeled NPs rarely exceeds 25 nm while real samples often reach a few hundred nm. Additionally, the strain rate in MD simulations is constrained to $10^{7-8}$ $s^{-1}$. Therefore, one has to clearly identify which mechanisms could depend on the size and strain rate. Dislocation nucleation is known to be rate and temperature sensitive due to its low activation volume ($\sim$1–10$b^3$). Zhu *et al.* have recently proposed an original method to address the probabilistic and thermally activated nature of dislocation nucleation.[42] The problem of size could also be solved using DD simulations including dislocation nucleation. Nevertheless, such an approach has not been applied to NPs.

### F. Route to DD

The dislocation nucleation processes observed in TEM or MD simulations can be reproduced within the elastic theory framework of dislocations.[166] For this reason, constitutive rules must be proposed at the scale of DD simulation and validated by comparison to experiments or lower scale simulations. Several attempts have already been made in the case of dislocation nucleation at free surfaces and applied with some success in thin films and large scale simulations.[167,168] It must be noticed that the existing solutions for the modeling of dislocation nucleation in DD simulations are not general and more work is required to propose better physically justified models.[169,170] Existing DD simulations, mainly on micropillars,

show that the standard cross-slip model initially developed for massive materials[171] are partially inadequate in simulations at the submicron scale.[172–174] Nevertheless, we know from MD simulation that cross-slip is partly modified at large stress and should be amended to account for new features existing close to free-surfaces.[175] Finally, the question of modeling the boundaries in DD simulation is not trivial. At least two solutions have been proposed in the past to solve the mechanical problem of free-surfaces, i.e., the question of the image force. One is the superposition method, and the other is based on the eigenstrain theory. Both solutions make use of a coupling between DD and FEM simulations and were successfully applied to micro- and nanomaterials.[176–178] The problem of dislocation-GB interactions is more complex. At a low stress level, the simplest solution considering grain boundary as a nonpenetrable interface is justified and was used with success in past studies.[179,180] The modeling of dislocation absorption and dislocation emission from GBs is more difficult and only simulation attempts have been made by considering simple low angle boundaries.[181,182]

## VI. FUTURE NANOMECHANICAL APPROACHES TO BRITTLENESS TRANSITIONS

Length scale effects on mechanical properties have a rich history, which emphasizes elasticity and plasticity.[183,184] Not until later studies did properties such as creep, corrosion, and fracture resistance become involved. This initially came about as a result of the demand for more computing power, which caused device scales to decrease over time as an inverse of Moore's law. As a result, fracture properties of thin film adhesion became heavily investigated,[185,186] such as delamination studies for the $10^2$ to $10^4$ nm scale around the year 2000.[187,188] These studies of adhered thin films were predominantly theoretical mechanics and experimental studies of indentation or bulge testing. Meanwhile, simultaneous advances in the analysis of strength properties revealed both indentation and nanopillar size effects.[139,189] While these addressed elasticity and plasticity, there was a lack of publications regarding fracture and ductile-to-brittle transitions (DBT). This absence was possibly due to the complexities of separate scale effects for both indentation and elastic–plastic cracks.[190,191]

For semibrittle materials, the complexities of length scale effects on elastic–plastic fracture prompted Cleri *et al.*[192] to apply large-scale atomistic computations to the problem. Their goal was to eliminate rigid body sliding as a mode of fracture. While this was nearly two decades ago, even today the agreement between simulation and experiment are marginal for materials like iron. Moller and Bitzek[193] evaluated the most common potentials for atomistic fracture simulations using the embedded atom method (EAM) and modified EAM. For eight different iron potentials, they concluded that there was too much variation of unstable stacking fault energies and the resulting $K_{IC}$ variation for emitting dislocations of 40% was far too large. However, use of other material simulation techniques,[194–197] mostly theoretical and applied mechanics, have produced some success, but are not often compared to the atomistic fundamentals. To achieve a more complete understanding of DBTs over multiple modeling scales, detailed *in situ* experiments measuring plastic and fracture properties of multiple materials are needed. Compared to iron, silicon is a more ideal material for DBT study from the perspective of lower dislocation densities, a higher temperature transition and wealth of available experimental data. This work will be focused entirely on silicon as a model material, especially for other semibrittle materials for which much of the discussion will be relevant.

It is our position that several experimental variables contribute to a controversy regarding how brittle silicon is at low temperatures, i.e., below 300 °C. These variables include state of stress (e.g., tension versus compression), doping type, dopant concentration, and size-based transitions at the nanometer scale.[198,199] These variables can affect fracture toughness by modifying dislocation character, nucleation, and mobility which shift the DBT temperature (DBTT) by hundreds of degrees. Recent studies from multiple disciplines, including geology,[200,201] physics,[202] civil engineering,[194] materials science,[147,203] and theoretical mechanics and applied mechanics,[192,193] have resulted in a consensus on what the key variables controlling the DBT are, but a comprehensive theory remains elusive. This is due to a lack of data needed to evaluate all the variables and their interactions. First, we will discuss the key variables regarding the DBT in silicon and frame the relevant experimental variables within this framework. Then, we will present some recent experimental findings on silicon and speculate on how they will contribute toward one day gathering the necessary data to systematically evaluate the DBT.

In Table I, we list what we consider the key variables are. There are so many that establishing an all-encompassing model has proven elusive for silicon and other semibrittle materials with DBTTs. The fracture toughness, $K_{IC}$, is related to the critical strain energy release rate, $G_{IC}$, which contains two types of energy dissipation due to the surface energy, $\gamma_s$, and plastic energy through $\gamma_{eff}$. The amount of plastic energy dissipation depends upon stress field interactions between the

TABLE I. DBT: key variables affecting flow and fracture.

| Symbol | Variable |
|---|---|
| b | The Burgers vector for full or partial dislocations occurring at the DBT |
| $\sigma_{ij}$ | The applied stress tensor governing pressure, plastic flow, and fracture |
| $\dot{\varepsilon}$ | The applied strain rate |
| T | The temperature |
| $H_0$ | An activation energy for dislocation nucleation or mobility |
| V | The dislocation velocity |
| E,$\nu$ | Appropriate elastic moduli and Poisson's ratio |
| $\gamma_s$ | Surface energy |
| $\gamma_{eff}$ | An effective "surface energy" which includes plastic energy dissipation |
| $G_{IC}$ | Strain energy release rate related to surface and plastic energies |
| $K_{IC}$ | Fracture toughness through $[E\ G_{IC}]^{1/2}$ |
| $V^*$ | Activation volume, same as an activation area times b |
| $\tau^*$ | An effective stress for dislocation nucleation or mobility |

crack tip and the emitted dislocations based upon the applied stress tensor, $\sigma_{ij}$. This stress field problem can then be related to $G_{IC}$ through the applied strain rate, $\dot{\varepsilon}$. Considering the interdependence of plasticity and fracture, the dislocation activation parameters V*, $\tau$*, $H_0$ can be combined to describe the dislocation velocity, v, as done in Hintsala *et al.*[204] to dictate the shielding of the crack tip by dislocations. The dislocation activation parameters will depend upon the temperature, T, and the presence of impurities. The dislocation shielding utilizes the stress field of each dislocation according to the Burgers vector, b, the elastic modulus, E, and Poisson's ratio, $\nu$.

Excellent progress has been made in understanding the high temperature (800 °C) DBT in silicon using phenomenological power laws that, when coupled to mechanics or atomistic simulations, give realistic representations.[195,198] However, the situation at higher stresses and lower temperatures, which are the common conditions at the nanoscale, is less certain. It is well known for silicon that dislocation character can be affected by temperature and chemistry, but whether this affects brittleness equally at all sizes and temperature regimes is not clear. Our view is that it is necessary to assess how experimental variables affect the above key variables in order to formulate a DBT model that does not depend on empirical constants. This requires understanding of how confining pressure,[205] radiation enhanced dislocation glide (REDG),[206] impurities,[207] state of stress,[208] and length scale[209] affect dislocation nucleation and mobility.

The REDG effect[204] is important since most studies of length scale effects at submicron sizes are accomplished in either SEM or TEM. Maeda *et al.*[206] observed from TEM experiments on SiC a roughly linear increase in dislocation velocities with increasing electron beam intensity, though the velocity depends on dislocation length and dislocation character. Similar observations have also been made for Si (Ref. 210) and GaAs.[211] We should point out, however, that some very small length scale studies of silicon nanospheres by both atomic force microscopy[134] and transmission electron microscopy[212] resulted in similar flow stress behavior. Considering dopant levels, extensive studies[205,213] have demonstrated that n-doping can favor enhanced dislocation velocities compared to intrinsic silicon. A similar effect was observed for p-doping at low strain rates and low temperatures by Brede and Haasen,[213] though at higher strain rates and temperatures it appeared to reverse.

Considering length scale effects, there have been numerous atomistic simulations such as the study by Kang and Cai.[209] They used a modified embedded-atom-method (MEAM) to study [110]-oriented silicon nanowires under tension with diameters of 2–7 nm, strain rates of $5 \times 108\ s^{-1}$, and temperatures of 100–1200 K. These simulations demonstrated that the [110] wires could undergo a DBTT at $d > 4$ nm but failed by ductile shear for smaller dimensions. They posed the question as to whether the DBT was controlled by dislocation mobility or dislocation nucleation. Clearly, for bulk silicon at high temperature, a strong case for dislocation velocity to be controlling DBT has been made.[198] However, at submicron length scales and low temperatures where extremely high stresses promote high dislocation velocities, there might be a transition to nucleation control. In terms of the activation volume, V*, there does appear to be such a transition which may correlate to such a change from velocity to nucleation control. For submicron sizes, we and others[214] have shown that the activation volume approaches 1 $b^3$ as shown in Fig. 5. It also appears that a fairly sharp transition occurs around 600 K, particularly for bulk behavior.[205] While one can hypothesize activation volumes less than 1 $b^3$, further exploration of this transition would enhance understanding of the DBT. This transition in activation volume likely signals a mechanism change affecting the activation volume-stress relationship for dislocation nucleation and/or mobility. These data are similar to the multiscale modeling of plastic deformation of molybdenum and tungsten.[195,215]

Further consideration of high stresses in metals by Gröger *et al.*[215] and silicon by Rabier and Demenet,[197,216] respectively, shows what happens to the dislocation core structure at high stresses. For example, Gröger *et al.*[215] demonstrated a very gradual change of V* at shear stresses of 400 to 800 MPa in Mo (close to the Peierl's stress) as V* $\sim$ 1 $b^3$ is approached. At these stress levels, the core structure could undergo complex changes that would affect the formation of kink pairs.[213] A dislocation core structure change could therefore further result in changes of the normal relationship between stress and activation volume. For silicon, this was suggested by Rabier *et al.*[197,216] more than a decade ago based upon *ex situ* weak-beam TEM imaging which showed full dislocations splitting into two a/6[112] partials, which they proposed to be based upon core structure changes under the applied 5 GPa confining pressure.

In a recent paper, using *in situ* deformation, we demonstrated that near-theoretical stresses of 12 GPa could be achieved in the initial stages of deforming dislocation-free nanocubes compressed along the [001] axis.[162] Continued deformation then dropped to 8 GPa, followed by strain hardening. In the early

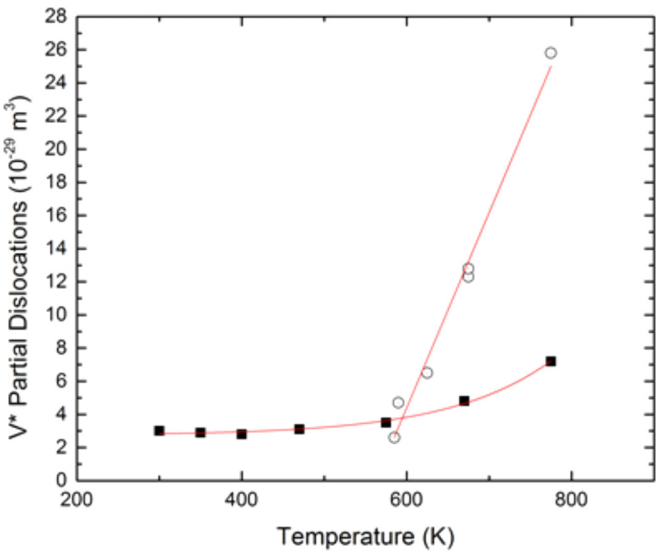


FIG. 5. (Color online) Activation volumes involving partial dislocations at very high stress (Ref. 212) and low temperatures in nanopillars (solid cube symbol) compared to bulk samples (open circle) at lower stress (Ref. 205).

stages, true stresses of 9 GPa formed following the load drop, and at the end, the true stress had strain hardened to at least 20 GPa. Based on this, it seems that high internal stress ($\gg$1 GPa) is responsible for the activation volume transition. This in turn would change the effective stress for continued plastic flow, which would be the applied stress minus the back stress from any trapped dislocations. The result of this is that the effective uniaxial stress state does not appear to exceed the theoretical true stress.

Last, we present preliminary data on fracture and speculate on how one might measure some of the parameters in Table I with which to better predict the DBTT in semibrittle materials theoretically. Previously, we had discussed indentation, sphere, and nanopillar evaluations in the size range of 30–1000 nm.[210] As all of these were in compression and fracture instabilities are generally associated with silicon in tension, the role of length scale is not totally addressed by these experiments. In a study of prenotched, bending fracture in an iron alloy just published,[217] ductile crack growth was observed in 100, 500, and 2500 nm thick beams under three-point bending conditions. We have since applied this to ⟨110⟩-oriented silicon beams. The 150 nm thick beam as shown in Fig. 6 was loaded *in situ* in an FEI F30 TEM operating at 300 keV with a Hysitron PI-95 PicoIndenter. Images were acquired aligned along the ⟨110⟩ zone axis with zero-loss filtering at 25 fps. The bending beam, shown unloaded in Fig. 6(b), was prenotched using the converged electron beam of the TEM to achieve a radius of curvature of only 2.5 nm. This was loaded up to the point in Fig. 6(c) just prior to crack initiation. The crack jump occurred within one

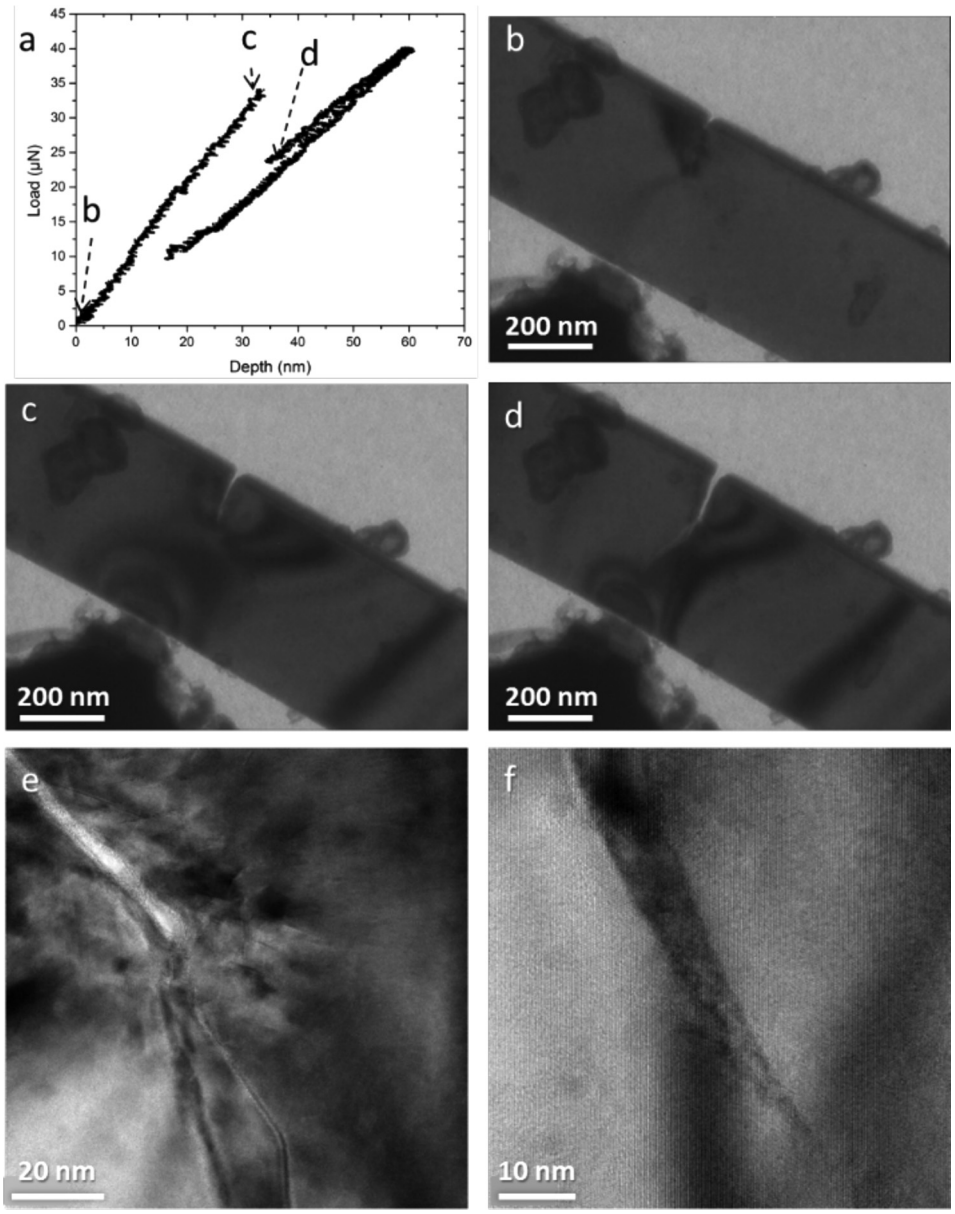


FIG. 6 (a) Load-displacement curve for a nominally 200 nm thick Si bending beam (b)–(d) *in situ* TEM video frames at (a) unloaded pretesting, (b) just before fracture, and (c) just after fracture. (e) and (f) Postmortem high resolution imaging of (e) base of the fabricated notch showing dislocations at the notch (f) after crack growth, indicating the crack tip is dislocation free. (g) Mesh utilized for FEM calculations and (h) the resulting applied stress intensity per unit applied force vs crack length.

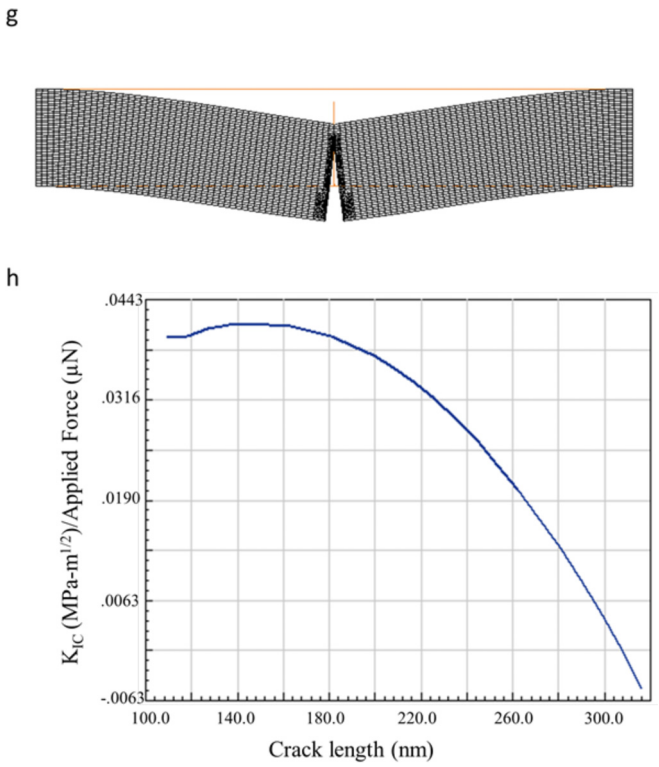


FIG. 6 (Color online) (*Continued.*)

frame, resulting in a load drop and crack arrest in Fig. 6(d). The crack can be observed to have deflected from the pre-notch at an angle ~35°, which is a reasonable match for a {111} cleavage plane projected onto the {110} surface of the bending beam. The initial notch length and beam height were 114 and 381 nm, respectively.

In order to account for loading complexities due to the clamping at the ends of the bending beam, FEM analysis was performed assuming isotropic values for E = 160 GPa and $\nu = 0.22$ utilizing the mesh shown in Fig. 6(g). The resulting fracture toughness, $K_{IC}$ per $\mu$N applied force versus the crack length based upon this FEM analysis is shown in Fig. 6(h). Based upon this analysis, the calculated fracture toughness was 1.33 MPa-m$^{1/2}$ at initiation in Fig. 6(c), which is a good match for other studies on submicron silicon. Note that this is well above the nominal 0.7 MPa m$^{1/2}$ found for bulk silicon single crystals. Based upon the strain energy release rates for this beam and bulk silicon, there is a factor of 3.6 increase in work per unit fracture area. There should be caution here as the dislocations associated with the notch fabrication may be producing some dislocation shielding as shown by postmortem high resolution imaging of the notch in Fig. 6(e). At arrest in Fig. 6(d), the calculated applied stress intensity was 0.57 MPa m$^{1/2}$ which compares reasonably well to the ideal fracture toughness of the {111} plane in Si of 0.62 MPa m$^{1/2}$ based upon a surface energy of 1.23 J/m$^2$. At the arrest point no dislocations were observed using high-resolution postmortem TEM in Fig. 6(f). Still, comparing this data to a previously published compressive data set,[212] gave an indication that such specimen types could be utilized in this length scale regime down to 100 nm thicknesses. The values indicated from Fig. 6 are lower than the previous compression data but still demonstrate a size effect.

Similar specimen types could be utilized with systematic exploration of variables of interest in order to determine their effects on the DBTT. For example, in progress are both activation energy and activation volume measurements as a function of temperature and strain rate. Next, evaluations of dopant levels or electron beam effects could be pursued. In principle, with an appropriate model, this would allow measurement of nearly all of the critical parameters that can also be accessed by atomistic simulations coupled to multiscale discretized dislocation models.

What we have shown here is the preliminary promise of *in situ* TEM and SEM evaluations of nano- and microscale samples that can supply needed parameters to better understand small-scale mechanical properties. This applies to properties measured at intermediate to near theoretical stresses, which govern both plasticity and fracture of semibrittle intermetallic, semiconductor, and ceramic crystals. While this is premature to being used for engineering applications, it is our position that all that is proposed is near at hand. The novelty is that sufficiently small volumes can be experimentally interrogated to give the type of physical parameters that will eventually be recoverable from atomistic simulations. To demonstrate this is possible, the following recent papers by Jaya *et al.*[218] and Best *et al.*[219] clearly demonstrate the experimental steps toward this goal. Expectantly, this will partially complete the path originally envisioned by St. John.[220]

## ACKNOWLEDGMENTS

J.W.K. gratefully acknowledges support from NSF CMMI-1437450 and NSF CMMI-1363093. A.M.M. acknowledges support from the Molecular Foundry at Lawrence Berkeley National Laboratory, U.S. Department of Energy under Contract No. DE-AC02-05H11231. I.S. gratefully acknowledges financial support from the U.S. Army Research Office under Grant No. W911NF-12-1-0548. E.T. gratefully acknowledges financial support from the National Science Foundation under Grant No. CMMI-1433887. J.A. is grateful to the Fédération Lyonnaise de Modélisation et Sciences Numériques (FLMSN), partner of the EQUIPEX EQUIP@MESO, which has provided access to HPC ressources for this work. The support of the research project Mera-FASS is acknowledged by B.D. E.H. and W.W.G. would like to acknowledge Claire Teresi for her assistance on *in situ* bend testing of silicon, Xie Yueyue for performing the Finite Element simulations presented here, and funding from NSF MRSEC and Hysitron, Inc. Sandia National Laboratories is a multiprogram laboratory managed and operated by Sandia Corporation, a wholly owned subsidiary of Lockheed Martin Corporation, for the U.S. Department of Energy's National Nuclear Security Administration under Contract No. DE-AC04-94AL85000.

[1]E. Pop, V. Varshney, and A. K. Roy, Mater. Res. Soc. Bull. **37**, 1273 (2012).
[2]Y. D. Kim *et al.*, Nat. Nanotechnol. **10**, 676 (2015).

[3]K. S. Novoselov, A. K. Geim, S. V. Morozov, D. Jiang, Y. Zhang, S. V. Dubonos, I. V. Grigorieva, and A. A. Firsov, Science **306**, 666 (2004).
[4]K. I. Bolotin, K. J. Sikes, Z. Jiang, M. Klima, G. Fudenberg, J. Hone, P. Kim, and H. L. Stormer, Solid State Commun. **146**, 351 (2008).
[5]C. R. Dean *et al.*, Nat. Nanotechnol. **5**, 722 (2010).
[6]C. Lee, X. Wei, J. W. Kysar, and J. Hone, Science **321**, 385 (2008).
[7]X. Wei and J. W. Kysar, Int. J. Solids Struct. **49**, 3201 (2012).
[8]K. F. Mak, C. Lee, J. Hone, J. Shan, and T. F. Heinz, Phys. Rev. Lett. **105**, 136805 (2010).
[9]R. C. Cooper, C. Lee, C. A. Marianetti, X. Wei, J. Hone, and J. W. Kysar, Phys. Rev. B **87**, 035423 (2013).
[10]A. K. Geim and I. V. Grigorieva, Nature **499**, 419 (2013).
[11]G.-H. Lee *et al.*, Science **340**, 1073 (2013).
[12]J. W. Kysar, Sci. Model. Simul. **15**, 143 (2008).
[13]X. Wei, B. Fragneaud, C. A. Marianetti, and J. W. Kysar, Phys. Rev. B **80**, 205407 (2009).
[14]M. Xu, A. Tabarraei, J. T. Paci, J. Oswald, and T. Belytschko, Int. J. Fract. **173**, 163 (2012).
[15]S. Kumar and D. M. Parks, Proc. R. Soc. London, A **471**, 2173 (2014).
[16]R. C. Cooper, C. A. Marianetti, and J. W. Kysar, Phys. Rev. B **90**, 167401 (2014).
[17]C. A. Marianetti and H. G. Yevick, Phys. Rev. Lett. **105**, 245502 (2010).
[18]C. Lee, X. Wei, Q. Li, R. Carpick, J. W. Kysar, and J. Hone, Phys. Status Solidi B **246**, 2562 (2009).
[19]S. Kumar and D. M. Parks, Nano Lett. **15**, 1503 (2015).
[20]H. S. Park and J. A. Zimmerman, Phys. Rev. B **72**, 054106 (2005).
[21]H. S. Park, K. Gall, and J. A. Zimmerman, Phys. Rev. Lett. **95**, 255504 (2005).
[22]X. W. Zhou, J. A. Zimmerman, E. D. Reedy, Jr., and N. R. Moody, Mech. Mater. **40**, 832 (2008).
[23]L. M. Hale, X. W. Zhou, J. A. Zimmerman, N. R. Moody, R. Ballarini, and W. W. Gerberich, J. Appl. Phys. **106**, 083503 (2009).
[24]G. J. Tucker, J. A. Zimmerman, and D. L. McDowell, Modell. Simul. Mater. Sci. Eng. **18**, 015002 (2010).
[25]G. J. Tucker, S. Tiwari, J. A. Zimmerman, and D. L. McDowell, J. Mech. Phys. Solids **60**, 471 (2012).
[26]L. Smith, J. A. Zimmerman, L. M. Hale, and D. Farkas, Modell. Simul. Mater. Sci. Eng. **22**, 045010 (2014).
[27]X. Zhou, D. K. Ward, B. M. Wong, F. P. Doty, and J. A. Zimmerman, J. Phys. Chem. C **116**, 17563 (2012).
[28]A. F. Voter, Phys. Rev. Lett. **78**, 3908 (1997).
[29]A. F. Voter, J. Chem. Phys. **106**, 4665 (1997).
[30]A. F. Voter, Phys. Rev. B **57**, R13985 (1998).
[31]D. Perez, B. P. Uberuaga, and A. F. Voter, Comput. Mater. Sci. **100**, 90 (2015).
[32]M. R. Sørensen and A. F. Voter, J. Chem. Phys. **112**, 9599 (2000).
[33]F. Montalenti and A. F. Voter, J. Chem. Phys. **116**, 4819 (2002).
[34]A. F. Voter, F. Montalenti, and T. C. Germann, Annu. Rev. Mater. Res. **32**, 321 (2002).
[35]Y. Mishin, A. Suzuki, B. P. Uberuaga, and A. F. Voter, Phys. Rev. B **75**, 224101 (2007).
[36]B. P. Uberuaga, D. Bacorisen, R. Smith, J. A. Ball, R. W. Grimes, A. F. Voter, and K. E. Sickafus, Phys. Rev. B **75**, 104116 (2007).
[37]B. P. Uberuaga, S. J. Stuart, and A. F. Voter, Phys. Rev. B **75**, 014301 (2007).
[38]R. A. Miron and K. A. Fichthorn, J. Chem. Phys. **119**, 6210 (2003).
[39]K. A. Fichthorn and S. Mubin, Comput. Mater. Sci. **100**, 104 (2015).
[40]B. P. Uberuaga, R. Smith, A. R. Cleave, G. Henkelman, R. W. Grimes, A. F. Voter, and K. E. Sickafus, Phys. Rev. B **71**, 104102 (2005).
[41]Y. Shim, V. Borovikov, B. P. Uberuaga, A. F. Voter, and J. G. Amar, Phys. Rev. Lett. **101**, 116101 (2008).
[42]T. Zhu, J. Li, A. Samanta, A. Leach, and K. Gall, Phys. Rev. Lett. **100**, 025502 (2008).
[43]T. Zhu and J. Li, Prog. Mater. Sci. **55**, 710 (2010).
[44]M. U. Bohner, J. Zeman, J. Smiatek, A. Arnold, and J. Kästner, J. Chem. Phys. **140**, 074109 (2014).
[45]L. D. Nguyen, K. L. Baker, and D. H. Warner, Phys. Rev. B **84**, 024118 (2011).
[46]T. J. Delph, P. Cao, H. S. Park, and J. A. Zimmerman, Modell. Simul. Mater. Sci. Eng. **21**, 025010 (2013).
[47]T. J. Delph and J. A. Zimmerman, "Transition saddle points and associated defects for a triaxially stretched FCC crystal" (unpublished).
[48]S. Pattamatta, R. S. Elliott, and E. B. Tadmor, Proc. Natl. Acad. Sci. **111**, E1678 (2014).
[49]K. R. Elder, M. Katakowski, M. Haataja, and M. Grant, Phys. Rev. Lett. **88**, 245701 (2002).
[50]K. R. Elder and M. Grant, Phys. Rev. E **70**, 051605 (2004).
[51]Y. Wang and J. Li, Acta Mater. **58**, 1212 (2010).
[52]P. Y. Chan, G. Tsekenis, J. Dantzig, K. A. Dahmen, and N. Goldenfeld, Phys. Rev. Lett. **105**, 015502 (2010).
[53]J. Berry, N. Provatas, J. Rottler, and C. W. Sinclair, Phys. Rev. B **86**, 224112 (2012).
[54]J. Berry, N. Provatas, J. Rottler, and C. W. Sinclair, Phys. Rev. B **89**, 214117 (2014).
[55]K. L. Baker and W. A. Curtin, Phys. Rev. B **91**, 014103 (2015).
[56]G.-M. Lu, Y.-L. Lu, T.-T. Hu, and Z. Chen, Comput. Mater. Sci. **106**, 170 (2015).
[57]J. Li, S. Sarkar, W. T. Cox, T. J. Lenosky, E. Bitzek, and Y. Wang, Phys. Rev. B **84** 054103 (2011).
[58]E. Dontsova, J. Rottler, and C. W. Sinclair, Phys. Rev. B **90**, 174102 (2014).
[59]E. Dontsova, J. Rottler, and C. W. Sinclair, Phys. Rev. B **91**, 224103 (2015).
[60]M. D. Uchic, P. A. Shade, and D. M. Dimiduk, Annu. Rev. Mater. Res. **39**, 361 (2009).
[61]Q. Yu, M. Legros, and A. M. Minor, MRS Bull. **40**, 62 (2015).
[62]M. D. Uchic, D. M. Dimiduk, J. N. Florando, and W. D. Nix, Science **305**, 986 (2004).
[63]N. Kheradmand, J. Dake, A. Barnoush, and H. Vehoff, Philos. Mag. **92**, 3216 (2012).
[64]D. Kiener and A. M. Minor, Nano Lett. **11**, 3816 (2012).
[65]P. Gumbsch and H. Gao, Science **283**, 965 (1999).
[66]A. J. Rosakis, O. Samudrala, and D. Coker, Science **284**, 1337 (1999).
[67]E. Faran and D. Shilo, Phys. Rev. Lett. **104**, 155501 (2010).
[68]M. R. Armstrong, B. W. Reed, B. R. Torralva, and N. D. Browning, Appl. Phys. Lett. **90**, 114101 (2007).
[69]W. E. King, G. H. Campbell, A. Frank, B. Reed, J. F. Schmerge, B. Siwick, B. C. Stuart, and P. W. Weber, J. Appl. Phys. **9**, 111101 (2005).
[70]M. Sennour, P. Laghoutaris, C. Guerre, and R. Molins, J. Nucl. Mater. **393**, 254 (2009).
[71]P. Laghoutaris, J. Chene, C. Guerre, O. Raquet, M. Sennour, R. Molins, F. Vaillant, and P. Scott, Energy Mater. **3**, 119 (2008).
[72]C. Guerre, P. Laghoutaris, J. Chene, L. Marchetti, R. Molins, C. Duhamel, and M. Sennour, "Stress corrosion cracking of alloy 600 in PWR primary water: Influence of chromium, hydrogen and oxygen diffusion," in *15th International Conference on Environmental Degradation* (2011).
[73]A. M. Minor, E. T. Lilleodden, E. A. Stach, and J. W. Morris, Jr., J. Electron. Mater. **31**, 958 (2002).
[74]J. Wang, J. Li, S. Yip, S. Phillpot, and D. Wolf, Phys. Rev. B **52**, 12627 (1995).
[75]M. Sob, L. G. Wang, and V. Vitek, Mater. Sci. Eng. A **234**, 1075 (1997).
[76]J. W. Morris and C. R. Krenn, Philos. Mag. A **80**, 2827 (2000).
[77]S. Ogata, J. Li, and S. Yip, Science **298**, 807 (2002).
[78]E. B. Tadmor, R. E. Miller, and R. S. Elliott, *Continuum Mechanics and Thermodynamics*: *From Fundamental Concepts to Governing Equations* (Cambridge University, Cambridge, 2012).
[79]I. Szlufarska, M. Chandross, and R. Carpick, J. Phys. D: Appl. Phys. **41**, 123001 (2008).
[80]K. L. Johnson, *Contact Mechanics* (Cambridge University, Cambridge, 1985).
[81]D. J. Maugis, Colloid Interface Sci. **150**, 243 (1992).
[82]B. N. J. Persson, J. Chem. Phys. **115**, 3840 (2001).
[83]C. Campana, M. H. Muser, and M. O. Robbins, J. Phys.: Condens. Matter **20**, 354013 (2008).
[84]E. B. Tadmor and R. E. Miller, *Modeling Materials: Continuum, Atomistic and Multiscale Techniques* (Cambridge University, Cambridge, 2011).
[85]H. Bhasharan *et al.*, Nat. Nanotechnol. **5**, 181 (2010).
[86]B. Q. Luan and M. O. Robbins, Nature **435**, 929 (2005).
[87]Y. Mo, K. T. Turner, and I. Szlufarska, Nature **457**, 1116 (2009).
[88]M. Mishra and I. Szlufarska, J. Mater. Sci. **48**, 1593 (2013).
[89]A. Li and I. Szlufarska, Phys. Rev. B **92**, 075418 (2015).
[90]M. H. Mueser and J. A. Harrison, Modell. Simul. Mater. Sci. Eng. **18**, 030201 (2010).

[91]Y. Qi and L. G. Hector, Phys. Rev B **69**, 235401 (2004).
[92]Y. Liu and I. Szlufarska, Phys. Rev. B **79**, 094109 (2009).
[93]G. Levita, E. Molinari, T. Polcar, and M. C. Righi, Phys. Rev B **92**, 085434 (2015).
[94]E. B. Tadmor, R. S. Elliott, J. P. Sethna, R. E. Miller, and C. A. Becker, JOM **63**, 17 (2011).
[95]M. Chandross, C. D. Lorenz, M. J. Stevens, and G. S. Grest, Langmuir **24**,1240 (2008).
[96]Y. Hu, T. Zhang, T. Ma, and H. Wang, Comput. Mater. Sci. **38**, 98 (2006).
[97]A. Schirmeisen, L. Jansen, H. Hölscher, and H. Fuchs, Appl. Phys. Lett. **88**, 123108 (2006).
[98]R. W. Carpick and M. Salmeron, Chem. Rev. **97**, 1163 (1997).
[99]A. Socoliuc, R. Bennewitz, E. Gnecco, and E. Meyer, Phys. Rev. Lett. **92**, 134301 (2004).
[100]E. B. Tadmor, R. Phillips, and M. Ortiz, Int. J. Solids Struct. **37**, 379 (2000).
[101]E. B. Tadmor, M. Ortiz, and R. Phillips, Philos. Mag. A **73**, 1529 (1996).
[102]V. B. Shenoy, R. Miller, E. B. Tadmor, D. Rodney, R. Phillips, and M. Ortiz, J. Mech. Phys. Solids **47**, 611 (1999).
[103]L. M. Dupuy, E. B. Tadmor, R. E. Miller, and R. Phillips, Phys. Rev. Lett. **95**, 060202 (2005).
[104]E. B. Tadmor, F. Legoll, W. K. Kim, L. M. Dupuy, and R. E. Miller, Appl. Mech. Rev. **65**, 010803 (2013).
[105]W. A. Curtin and R. E. Miller, Modell. Simul. Mater. Sci. Eng. **11**, R33 (2003).
[106]R. E. Miller and E. B. Tadmor, Modell. Simul. Mater. Sci. Eng. **17**, 053001 (2009).
[107]Q. Li, Y. Dong, D. Perez, A. Martini, and R. W. Carpick, Phys. Rev. Lett. **106**, 126101 (2011).
[108]W. K. Kim and M. L. Falk, Modell. Simul. Mater. Sci. Eng. **18**, 034003 (2010).
[109]Y. Liu and I. Szlufarska, Phys. Rev. Lett. **109**, 186102 (2012).
[110]I. Barel, M. Urbakh, L. Jansen, and A. Schirmeisen, Phys. Rev. Lett. **104**, 066104 (2010).
[111]L. Bocquet and J. L. Barrat, Phys. Rev. E **49**, 3079 (1994).
[112]K. Huang and I. Szlufarska I, Phys. Rev. E **89**, 032119 (2014).
[113]W. K. Kim, M. Luskin, D. Perez, A. F. Voter, and E. B. Tadmor, J. Mech. Phys. Solids **63**, 94 (2014).
[114]W. K. Kim and E. B. Tadmor, "Spatial and temporal multiscale simulation of nanoindentation using hyper–QC" (unpublished).
[115]H. G. Craighead, Science **290**, 1532 (2000).
[116]P. Alivisatos, Nat. Biotechnol. **22**, 47 (2003).
[117]D. Mordehai, S.-W. Lee, B. Backes, D. J. Srolovitz, W. D. Nix, and E. Rabkin, Acta Mater. **59**, 5202 (2011).
[118]C. E. Carlton and P. J. Ferreira, Micron **43**, 1134 (2012).
[119]R. Maaß, L. Meza, B. Gan, S. Tin, and J. R. Greer, Small **8**, 1869 (2012).
[120]W.-Z. Han *et al.*, Adv. Mater. **27**, 3385 (2015).
[121]I. Issa, J. Amodeo, J. Réthoré, L. Joly-Pottuz, C. Esnouf, J. Morthomas, M. Perez, J. Chevalier, and K. Masenelli-Varlot, Acta Mater. **86**, 295 (2015).
[122]J. Deneen and C. B. Carter, J. Mater. Sci. **44**, 2408 (2009).
[123]W. W. Gerberich *et al.*, J. Mech. Phys. Solids **51**, 979 (2003).
[124]L. M. Hale, X. Zhou, J. A. Zimmerman, N. R. Moody, R. Ballarini, and W. W. Gerberich, Comput. Mater. Sci. **50**, 1651 (2011).
[125]P. Valentini, W. Gerberich, and T. Dumitrica, Phys. Rev. Lett. **99**, 175701 (2007).
[126]N. Zhang *et al.*, J. Appl. Phys. **109**, 063534 (2011).
[127]M. Mačković, F. Niekiel, L. Wondraczek, and E. Spiecker, Acta Mater. **79**, 363 (2014).
[128]A. S. Barnard and P. Zapol, J. Chem. Phys. **121**, 4276 (2004).
[129]M. J. Sweet, A. Chesser, and I. Singleton, Adv. Appl. Microbiol. **80**, 113 (2012).
[130]J. Li, Z. Shan, and E. Ma, MRS Bull. **39**, 108 (2014).
[131]H. Liang, M. Upmanyu, and H. Huang, Phys. Rev. B **71**, 241403 (2005).
[132]M. T. McDowell, A. M. Leach, and K. Gall, Nano Lett. **8**, 3613 (2008).
[133]R. Dingreville and J. Qu, J. Mech. Phys. Solids **53**, 1827 (2005).
[134]J. Cai, Y.-D. Wang, and Z.-W. Huang, Modell. Simul. Mater. Sci. Eng. **21**, 035010 (2013).
[135]W. M. Mook, J. D. Nowak, C. R. Perrey, C. B. Carter, R. Mukherjee, S. L. Girshick, P. H. McMurry, and W. W. Gerberich, Phys. Rev. B **75**, 214112 (2007).
[136]C. Gerard and L. Pizzagalli, Pramana J. Phys. **84**, 1041 (2015).
[137]H. Bei, S. Shim, G. M. Pharr, and E. P. George, Acta Mater. **56**, 4762 (2008).
[138]S. I. Rao, D. M. Dimiduk, T. A. Parthasarathy, M. D. Uchic, M. Tang, and C. Woodward, Acta Mater. **56**, 3245 (2008).
[139]T. A. Parthasarathy, S. I. Rao, D. M. Dimiduk, M. D. Uchic, and D. R. Trinkle, Scr. Mater. **56**, 313 (2007).
[140]J. R. Greer, W. C. Oliver, and W. D. Nix, Acta Mater. **53**, 1821 (2005).
[141]V. G. Gryaznov, A. M. Kaprelov, and A. E. Romanov, Scr. Mater. **23**, 1443 (1989).
[142]P. Hirel, S. Brochard, L. Pizzagalli, and P. Beauchamp, Scr. Mater. **57**, 1141 (2007).
[143]S. Brochard, P. Hirel, L. Pizzagalli, and J. Godet, Acta Mater. **58**, 4182 (2010).
[144]H. Van Swygenhoven, P. M. Derlet, and A. G. Frøseth, Nat. Mater. **3**, 399 (2004).
[145]M. Chen, E. Ma, K. J. Hemker, H. Sheng, Y. Wang, and X. Cheng, Science **300**, 1275 (2003).
[146]A. Sedlmayr, E. Bitzek, D. Gianola, G. Richter, R. Mönig, and O. Kraft, Acta Mater. **60**, 3985 (2012).
[147]J. Amodeo, C. Begau, and E. Bitzek, Mater. Res. Lett. **2**, 140 (2014).
[148]F. Östlund, K. Rzepiejewska-Malyska, K. Leifer, L. M. Hale, Y. Tang, R. Ballarini, W. W. Gerberich, and J. Michler, Adv. Funct. Mater. **19**, 2439 (2009).
[149]S. Korte, J. S. Barnard, R. J. Stearn, and W. J. Clegg, Int. J. Plast. **27**, 1853 (2011).
[150]K. Kendall, Nature **272**, 710 (1978).
[151]C. L. Johnson, E. Snoeck, M. Ezcurdia, B. Rodríguez-González, I. Pastoriza-Santos, L. M. Liz-Marzán, and M. J. Hÿtch, Nat. Mater. **7**, 120 (2007).
[152]M. R. Langille, J. Zhang, M. L. Personick, S. Li, and C. A. Mirkin, Science **337**, 954 (2012).
[153]P. J. Imrich, C. Kirchlechner, D. Kiener, and G. Dehm, Scr. Mater. **100**, 94 (2015).
[154]Y. Kim, S. Lee, J. B. Jeon, Y.-J. Kim, B.-J. Lee, S. H. Oh, and S. M. Han, Scr. Mater. **107**, 5 (2015).
[155]N. Kheradmand, H. Vehoff, and A. Barnoush, Acta Mater. **61**, 7454 (2013).
[156]S. Lefebvre, B. Devincre, P. Aubert, and T. Hoc, Philos. Mag. A **94**, 2472 (2014).
[157]J. Bian, X. Niu, H. Zhang, and G. Wang, Nanoscale Res. Lett. **9**, 335 (2014).
[158]K. Lu, L. Lu, and S. Suresh, Science **324**, 349 (2009).
[159]Y. M. Wang, Nat. Mater. **12**, 697 (2013).
[160]M. Chassagne, M. Legros, and D. Rodney, Acta Mater. **59**, 1456 (2011).
[161]Z. H. Jin, P. Gumbsch, K. Albe, E. Ma, K. Lu, H. Gleiter, and H. Hahn, Acta Mater. **56**, 1126 (2008).
[162]J. Guénolé, J. Godet, and S. Brochard, Phys. Rev. B **87**, 045201 (2013).
[163]A. J. Wagner, E. D. Hintsala, P. Kumar, W. W. Gerberich, and K. A. Mkhoyan, Acta Mater. **100**, 256 (2015).
[164]K. Zheng *et al.*, Nat. Commun. **1**, 24 (2010).
[165]R. Soler and J. M. Aldareguia, Adv. Eng. Mater. **14**, 1004 (2012).
[166]I. J. Beyerlein, M. J. Demkowicz, A. Misra, and B. P. Uberuaga, Prog. Mater. Sci **74**, 125 (2015).
[167]M. Grydlik, F. Boioli, H. Groiss, R. Gatti, M. Brehm, F. Montalenti, B. Devincre, F. Schäffler, and L. Miglio, Appl. Phys. Lett. **101**, 013119 (2012).
[168]H.-J. Chang, M. Fivel, D. Rodney, and M. Verdier, C. R. Phys. **11**, 285 (2010).
[169]A. T. Jennings, C. R. Weinberger, S.-W. Lee, Z. H. Aitken, L. Meza, and J. R. Greer, Acta Mater. **61**, 2244 (2013).
[170]S. Aubry, K. Kang, S. Ryu, and W. Cai, Scr. Mater. **64**, 1043 (2011).
[171]L. P. Kubin, G. Canova, M. Condat, B. Devincre, V. Pontikis, and Y. Brechet, Solid State Phenom. **23–24**, 455 (1992).
[172]A. M. Hussein, S. I. Rao, M. D. Uchic, D. M. Dimiduk, and J. A. El-Awady, Acta Mater. **85**, 180 (2015).
[173]M. Stricker and D. Weygand, Acta Mater. **99**, 130 (2015).
[174]I. Ryu, W. D. Nix, and W. Cai, Acta Mater. **61**, 3233 (2013).
[175]S. I. Rao, D. M. Dimiduk, T. A. Parthasarathy, M. D. Uchic, and C. Woodward, Acta Mater. **61**, 2500 (2013).
[176]Y. Cui, Z. Liu, and Z. Zhuang, Int. J. Plast. **69**, 54 (2015).
[177]J. C. Crone, P. W. Chung, K. W. Leiter, J. Knap, S. Aubry, G. Hommes, and A. Arsenlis, Modell. Simul. Mater. Sci. Eng. **22**, 035014 (2014).
[178]A. Vattré, B. Devincre, F. Feyel, R. Gatti, S. Groh, O. Jamond, and A. Roos, J. Mech. Phys. Solids **63**, 491 (2014).

[179]C. de Sensal, B. Devincre, and L. P. Kubin, Key Eng. Mater. **423**, 25 (2009).
[180]C. Zhou and R. LeSar, Int. J. Plast. **30–31**, 185 (2012).
[181]B. Liu, P. Eisenlohr, F. Roters, and D. Raabe, Acta Mater. **60**, 5380 (2012).
[182]G. V. P. Reddy, C. Robertson, C. Déprés, and M. Fivel, Acta Mater. **61**, 5300 (2013).
[183]J. W. Hutchinson and Z. Suo, Adv. Appl. Mech. **29**, 63 (1991).
[184]S. S. Chiang, D. B. Marshall, and A. G. Evans, J. Appl. Phys. **53**, 298 (1982).
[185]M. P. De Boer and W. W. Gerberich, Acta Mater. **44**, 3169 (1996).
[186]X. Li and B. Bhushan, Surf. Coat. Technol. **163**, 521 (2003).
[187]R. H. Dauskardt, M. Lane, Q. Ma, and N. Krishna, Eng. Fract. Mech. **61**, 141 (1998).
[188]A. A. Volinsky, J. B. Vella, and W. W. Gerberich, Thin Solid Films **429**, 201 (2003).
[189]W. D. Nix and H. Gao, J. Mech. Phys. Solids **46**, 411 (1998).
[190]A. G. Evans, M. D. Drory, and M. S. Hu, J. Mater. Res. **3**, 1043 (1998).
[191]M. R. Begley and J. W. Hutchinson, J. Mech. Phys. Solids **46**, 2049 (1998).
[192]F. Cleri, S. R. Phillpot, D. Wolf, and S. Yip, J. Am. Ceram. Soc. **81**, 501 (1998).
[193]J. J. Möller and E. Bitzek, Modell. Simul. Mater. Sci. **22**, 045002 (2014).
[194]J. W. Hutchinson, Int. J. Solids Struct. **37**, 225 (2000).
[195]R. Ramachandramoorthy, R. Bernal, and H. D. Espinosa, ACS Nano **9**, 4675 (2015).
[196]M. J. Buehler, A. C. T. van Duin, and W. A. Goddard III, Phys. Rev. Lett. **99**, 165502 (2007).
[197]E. Bitzek and P. Gumbsch, Acta Mater. **61**, 1394 (2013).
[198]M. S. R. N. Kiran, T. T. Tran, L. A. Smillie, B. Haberl, D. Subianto, J. S. Williams, and J. E. Bradby, J. Appl. Phys. **117**, 205901 (2015).
[199]J. Rabier, L. Pizzagalli, and J. L. Demenet, Dislocat. Solids **16**, 47 (2010).
[200]P. B. Hirsch and S. G. Roberts, Philos. Trans. R. Soc. A **355**, 1991 (1997).
[201]D. L. Goldsby and T. E. Tullis, Geophys. Res. Lett. **29**, 25, doi:10.1029/2002GL015240 (2002).
[202]M. S. Duesbery, B. Joos, and D. J. Michel, Phys. Rev. B **43**, 5143 (1991).
[203]W. Kang and M. T. A. Saif, Adv. Funct. Mater. **23**, 713 (2013).
[204]E. Hintsala, C. Teresi, A. J. Wagner, K. A. Mkhoyan, and W. W. Gerberich, J. Mater. Res. **29**, 1513 (2014).
[205]J. Rabier, P. Cordier, J. L. Demenet, and, H. Garem, Mater. Sci. Eng. A **309**, 74 (2001).
[206]K. Maeda, K. Suzuki, and M. Ichihara, Micros. Microanal. Microstruct. **4**, 211 (1993).
[207]A. George and G. Champier, Phys. Status Solidi A **53**, 529 (1979).
[208]K. Shima, S. Izumi, and S. Sakai, J. Appl. Phys. **108**, 063504 (2010).
[209]K. Kang and W. Cai, Int. J. Plast. **26**, 1387 (2010).
[210]H. R. Kolar, J. C. H. Spence, and H. Alexander, Phys. Rev. Lett. **77**, 4031 (1996).
[211]K. Maeda and S. Takeuchi, Jpn. J. Appl. Phys., Part 2 **20**, L165 (1981).
[212]A. R. Beaber, J. D. Nowak, O. Ugurlu, W. M. Mook, S. L. Girshick, R. Ballarini, and W. W. Gerberich, Philos. Mag. **91**, 1179 (2011).
[213]M. Brede and P. Haasen, Acta Metall. **36**, 2003 (1988).
[214]J. Rabier, A. Montagne, J. M. Wheeler, J. L. Demenet, J. Michler, and R. Ghisleni, Phys. Status Solidi C **10**, 11 (2013).
[215]R. A. Gröger, G. Bailey, and V. Vitek, Acta Mater. **56**, 5401 (2008).
[216]J. Rabier and J. L. Demenet, Scr. Mater. **45**, 1259 (2001).
[217]E. Hintsala, D. Kiener, J. Jackson, and W. W. Gerberich, Exp. Mech. **55**, 1681 (2015).
[218]B. N. Jaya, J. M. Wheeler, J. Wehrs, J. P. Best, R. Soler, J. Michler, C. Kirchlechner, and G. Dehm, Nano Lett. **16**, 7597 (2016).
[219]J. P. Best, J. Zechner, J. M. Wheeler, R. Schoeppner, M. Morstein, and J. Michler, Philos. Mag. **96**, 3552 (2016).
[220]C. St. John, Philos. Mag. **32**, 1193 (1975).